LUND UNIVERSITY

Quality Assurance in Radiotherapy - Development and evaluation of new tools for improved patient safety

Nordström, Fredrik

2012

Quality Assurance in Radiotherapy

Development and evaluation of new tools for improved patient safety in external beam therapy

Fredrik Nordström

Medical Radiation Physics
Faculty of Science
Lund University
Malmö 2012

Quality Assurance in Radiotherapy

Development and evaluation of new tools for improved patient safety in external beam therapy

LUND
UNIVERSITY

Fredrik Nordström
Malmö 2012

Department of Medical Radiation Physics
Faculty of Science
Lund University
ISBN 978-91-7473-271-9

Printed in Sweden by Media-Tryck, Lund University
Lund 2012

Abstract

Preparation for radiotherapy is a complex procedure that involves many different technologies and groups of professionals. The rapid development and introduction of new technologies throughout the last decade have made it possible to deliver highly conformal, individually-shaped dose distributions with high accuracy. However, there is widespread concern that current quality assurance practices have not been updated at the pace necessary to provide adequate and cost-effective safeguards against treatment delivery errors.

The overall aim of this thesis was to develop and evaluate new, efficient tools for patient-specific quality assurance of the radiotherapy process, including the following areas: transfer of information, independent monitor unit verification, pre-treatment measurements, *in vivo* dosimetry, and end-to-end tests.

Within the framework of the thesis, a concept for ensuring data integrity was proposed and used to compare different combinations of treatment planning systems and record-and-verify systems with respect to data integrity. Because the concept is based on the Digital Imaging and Communications in Medicine (DICOM) global information standard, it is generally applicable to most radiotherapy computer systems. Additionally, a software for monitor unit verifications was developed, and the tools within Statistical Process Control were used to analyse calculation results from this software in a multicentre study. Time-resolved dosimetry systems were developed and applied to pre-treatment measurements and *in vivo* dosimetry, allowing rigorous analysis of the accuracy of the treatment planning and delivery systems and forming a basis for real-time *in vivo* dosimetry. Finally, gel dosimetry and anthropomorphic phantoms were demonstrated to provide important tools for complete end-to-end tests.

The tools developed in this thesis have two important applications: routine use in daily clinical practice, and when introducing new technologies in the local clinical setting. The proposed methods and concepts can improve patient safety and reduce the resources required for a comprehensive quality assurance program.

Popular scientific summary in Swedish

Strålbehandling är en av de vanligaste behandlingarna mot cancer. Hälften av alla behandlingar syftar till att bota patienten från sjukdomen, men strålbehandling är även en mycket effektiv behandling för att lindra smärta och andra symptom för patienter med en obotlig cancer.

Förberedelse inför strålbehandling är en komplicerad procedur, som innefattar många olika tekniska system och yrkeskategorier. Det är därför inte ovanligt att fel uppkommer i denna process. Världshälsoorganisationen (WHO) har rapporterat att risken för en enskild patient att drabbas av ett fel med milda till lindriga konsekvenser är ungefär 0.15%. Motsvarande risk för fel med allvarliga konsekvenser är mellan 50 och 100 per miljon behandlingar.

Den snabba utvecklingen och introduktionen av ny teknik under det senaste decenniet har gjort det möjligt att ge behandlingar med hög noggrannhet. Detta medför att en hög stråldos kan ges till tumören, medan frisk vävnad skonas. De nya komplicerade teknikerna för planering och leverans av behandlingen kan även ha skapat en miljö med större sannolikhet för fel. Paradoxalt nog kan teknik för att öka noggrannheten även vara en ny källa till fel om den inte används korrekt.

För att reducera sannolikheten för fel är omfattande kvalitetssäkringssystem en del av strålterapiprocessen på moderna strålterapikliniker. Dessa system reducerar risken för olyckor och fel, samtidigt som de ökar sannolikheten att tidigt upptäcka de fel som ändå uppkommer och reducerar därmed konsekvenserna för patienten. Det finns dock en allmän oro att dagens kvalitetssäkringsprogram inte utgör ett adekvat och kostnadseffektivt skydd mot fel i behandlingar på grund av den snabba tekniska utvecklingen och introduktionen av nya behandlingstekniker.

Inom ramen för denna avhandling har nya effektiva verktyg utvecklats och utvärderats för att säkerställa att korrekta behandlingsparametrar används. En implementering av dessa verktyg, i det dagliga arbetet med att leverera högkvalitativa behandlingar, kan förbättra säkerheten för den enskilda patienten.

Abbreviations

3D-CRT	Three-dimensional conformal radiotherapy
AAA	Anisotropic analytical algorithm
AAPM	American Association of Physicists in Medicine
CNS	Central nervous system
CT	Computed tomography
DICOM	Digital Imaging and Communications in Medicine
DICOM-RT	DICOM radiotherapy extension
DRR	Digitally reconstructed radiograph
EM	Electromagnetic
EPID	Electronic portal imaging device
ESTRO	European Society for Therapeutic Radiology and Oncology
IAEA	International Atomic Energy Agency
IGRT	Image-guided radiotherapy
IMRT	Intensity-modulated radiotherapy
MLC	Multileaf collimator
MRI	Magnetic resonance imaging
MU	Monitor unit
nPAG	Normoxic polyacrylamide gel
OAR	Organ at risk
PBC	Pencil beam convolution
PMMA	Polymethyl methacrylate
QC	Quality control
QA	Quality assurance
RVP	Radiotherapy verification program
SPC	Statistical process control
SPR	Scatter-to-primary ratio
TCP	Tumour control probability
TPS	Treatment planning system
WHO	World Health Organization
VMAT	Volumetric modulated arc therapy

Original papers

This thesis is based on the following papers, which are referred to in the text by their respective Roman numerals.

I. *Ensuring the integrity of treatment parameters throughout the radiotherapy process*
Nordström F, Ceberg C, Bäck SÅJ
Radiotherapy and Oncology (2012), doi:10.1016/j.radonc.2012.01.004

II. *Control chart analysis of data from a multicenter monitor unit verification study*
Nordström F, af Wetterstedt S, Johnsson S, Ceberg C, Bäck SÅJ
Radiotherapy and Oncology 102 (2012) 364-370

III. *4D dosimetric verification of VMAT treatments*
Nordström F, af Wetterstedt S, Ceberg C, Bäck SÅJ
Manuscript submitted to Medical Physics

IV. *Real-time in vivo dosimetry and target localization during VMAT prostate treatments*
Nordström F, Ravkilde T, Poulsen PR, Jönsson M, Ceberg C, Bäck SÅJ
Manuscript submitted to Radiotherapy and Oncology

V. *3D geometric gel dosimetry verification of intraprostatic fiducial guided hypofractionated radiotherapy of prostate cancer*
Nordström F, Ceberg S, af Wetterstedt S, Nilsson P, Ceberg C, Bäck SÅJ
Journal of Physics: Conference Series 250 (2010) 012059

Preliminary reports

The following preliminary reports were presented at international meetings and conferences.

Intensity Modulated Radiotherapy dose verification methods; an intercomparison study. Nordström *et al.*, Abstract and poster at 9th Biennial ESTRO Meeting on Physics and Radiation Technology for Clinical Radiotherapy (2007), Barcelona, Spain.

Development and evaluation of a method to verify the integrity of treatment data throughout the radiotherapy process. Nordström *et al.*, Abstract and poster at ESTRO 27 (2008), Göteborg, Sweden.

Patient specific IMRT verification using an independent dose calculation method and anatomical data. Nordström *et al.*, Abstract and poster at the 10th Biennial ESTRO Meeting on Physics and Radiation Technology for Clinical Radiotherapy (2009), Maastricht, The Netherlands.

3D geometric gel dosimetry verification of intraprostatic fiducial guided hypofractionated radiotherapy of prostate cancer. Nordström *et al.*, Abstract and oral presentation at The 6th International Conference on 3D Radiation Dosimetry (2010), Hilton Head Island, U.S.A.

Control chart analysis of data from a national monitor unit verification study. Nordström *et al.*, Abstract and oral presentation at ESTRO 29 (2010), Barcelona, Spain.

Quality assurance methods in radiotherapy. Nordström *et al.*, Invited speaker at Medical Physics in the Baltic States (2010), Kaunas, Lithuania.

Table of contents

1 Introduction

Radiotherapy is one of the main modalities for the treatment of cancer. According to the best available evidence, 52% of patients with cancer should receive external beam radiotherapy at least once during the treatment of their disease (Delaney *et al.* 2005). Approximately 54% of these treatments are delivered with the intent to cure the patient (SBU 2003). Radiotherapy is also a highly effective treatment option to alleviate pain and control other symptoms in cases of advanced or recurrent cancer (WHO 2008).

The aim of radiotherapy treatment planning is to maximise the ratio between the tumour control probability (TCP) and the normal tissue complications probability, i.e. the therapeutic ratio. This ratio has been continuously increased by the introduction of improved treatment delivery techniques, more advanced treatment planning systems (TPSs), and the employment of new imaging modalities to localise and delineate tumours and organs at risk (OARs).

In three-dimensional conformal radiotherapy (3D-CRT), the radiation target (e.g., the primary tumour volume with an additional margin) and the OARs are delineated from patient-specific 3D image data sets. The images can be acquired through different modalities, including computed tomography (CT), magnetic resonance imaging (MRI), positron emission tomography, and ultrasound. CT images also contain information about Hounsfield units; converted into electron density distributions, they form a basis for sophisticated absorbed dose calculations in the TPS.

Intensity-modulated radiotherapy (IMRT) is an efficient method for generating dose distributions with improved conformity to the target volumes and reduced absorbed doses to the OARs compared with the 3D-CRT technique. IMRT is based on the use of intensity-modulated radiation beams and computerised iterative plan optimisations. The intensity-modulated beams are delivered at static gantry angles, usually by varying the position of the individual leaves of the multileaf collimator (MLC). Volumetric modulated arc therapy (VMAT) provides additional degrees of freedom by allowing the gantry to rotate during radiation delivery, while the speed and the dose rate are varied.

Preparation of radiotherapy is a complex procedure that involves many different technologies and groups of professionals. A high level of accuracy in all steps of the process is required in order to deliver treatments that result in high TCP and minimal risk to normal tissue. The literature suggests an overall accuracy requirement of 2.5-3.5% (1 s.d.) (Brahme 1984, Goitein 1983, IAEA 2000a, Mijnheer *et al.* 1987).

Radiotherapy-related errors are not uncommon, and the risk of mild to moderate injuries from radiotherapy errors is approximately 0.15% per treatment course (Shafiq *et al.* 2009, WHO 2008). The risk of serious injuries is between 50 and 100 per million treatment courses (Munro 2007). This risk is 80-170 times higher than the risk of a fatal accident in commercial aviation per departure (0.6 per million departures) (ICAO 2011). Many errors are also likely to go undetected, especially if they result in underdosage. These errors can also cause adverse effects (i.e., local recurrence) (Ash and Bates 1994).

The rapid development and introduction of new technology during the last decade has made it possible to deliver highly conformal, individually-shaped dose distribution with high accuracy. However, the increased complexity of treatment planning and treatment delivery may have created an environment with a greater probability of incidents (Huang *et al.* 2005, WHO 2008). Technologies introduced to increase the accuracy of treatments might also act as a new source of error if they are not used correctly (Patton *et al.* 2003).

Quality assurance (QA) programs are integral components of modern radiation therapy practice (IAEA 2005, Saw *et al.* 2008). They reduce the likelihood of accidents and errors; in addition, by increasing the probability of early detection of the errors that do occur, the consequences for the patients are reduced. However, because of the rapid implementation of new technologies, there is widespread concern that current QA programs do not provide adequate or cost-effective safeguards against treatment delivery errors (Saw *et al.* 2008).

1.1 Aims of this thesis

The overall aim of this thesis was to develop and evaluate new, efficient tools for patient-specific QA of the physical aspects of the radiotherapy process. The following areas within the concept of independent checking were prioritised based on international reports and publications (DOH 2007, IAEA 2000b, RCR 2008, WHO 2008):

- Transfer of information
- Independent monitor unit (MU) verification
- Pre-treatment measurements
- *In vivo* dosimetry
- End-to-end tests

Derived from the general aim, the following detailed objectives were formulated:

- To develop and evaluate a method based on the Digital Imaging and Communications in Medicine (DICOM) global information standard to ensure data integrity when transferring information between systems.
- To investigate the verification process of the TPS calculated MU:s using an independent calculation algorithm and statistical process control (SPC).
- To develop tools for time-resolved dosimetry and investigate its application to pre-treatment and real-time *in vivo* verification of VMAT treatments.
- To investigate the feasibility of polymer gel dosimetry to audit treatments, using gold fiducial markers for image guidance.

2 Radiotherapy risks

To avoid adverse events in radiotherapy, it is important to learn from errors that have occurred previously (Holmberg 2007). Lessons learned from incidents can aid the identification of potential problems and the correction of deficiencies in the local clinical setting (IAEA 2005). Preventive actions based on lessons learned should be applied systematically as a part of the QA program (IAEA 2005, RCR 2008).

When identifying the contributing factors of a large number of incidents, patterns becomes evident (Cunningham *et al.* 2010, Shafiq *et al.* 2009, WHO 2008). The World Health Organization (WHO) has reported that the greatest bulk of radiotherapy-related incidents without any harm to the patient (38%) are related to misinformation or errors in data transfer (Shafiq *et al.* 2009, WHO 2008). Ten percent of all reported major radiotherapy incidents, analysed in the same study, occurred during information transfer. Human mistakes or inattention were the main reasons for transcription errors, rounding errors, forgotten data, and interchange of data. In addition, data might be lost or misinterpreted because different systems may not fully support the same data structures of the information standards used for information transfer (Swerdloff 2007).

Independent checking is an important intervention to reduce risks associated with many steps of the radiotherapy process (WHO 2008). The simplest form of independent checking is to have two workers verify the same parameter independently of each other. A more advanced form of independent checking in radiotherapy is the verification of the TPS calculated MU:s using an independent calculation algorithm. When errors occur, they are often repeated many times before they are finally detected (Cunningham *et al.* 2010, DOH 2007). The errors are often discovered by chance, rather than by quality control (QC) methods (DOH 2007). *In vivo* dosimetry during the first fraction of radiotherapy increases the likelihood that errors will be detected early (Calandrino *et al.* 1997, Lanson *et al.* 1999, Noel *et al.* 1995). However, *in vivo* dosimetry programs have not been widely implemented owing to their associated costs (Essers and Mijnheer 1999). Another approach is the use of pre-treatment control measurements, in which the absorbed dose from a dummy run conducted in the absence of the patient are verified. Pre-treatment

control measurements can avoid exposing the patient to a first-time error (DOH 2007).

Another commonly reported cause of errors is lack of training of healthcare professionals when new technologies are introduced (DOH 2007). Competency certification has been identified as another important intervention to reduce risks (WHO 2008).

In this thesis, three recent major accidents (summarised in this chapter) have been considered of special importance because of the many lessons that can be learned from them. They are referred to within the context of QA, and have been used extensively as examples that a comprehensive QA program should render detectable.

2.1 Unsaved MLC control points

In March 2005, a patient receiving treatment for cancer located at the base of the tongue was fatally overexposed at St. Vincent's Hospital in New York. Instead of receiving the prescribed absorbed dose of 2 Gy per fraction, 13-14 Gy per fraction were administered during three fractions to a volume between the larynx and the base of the skull.

The patient's treatment was initiated on an inadequate 5-field sliding-window IMRT plan that had been properly verified using electronic portal imaging device (EPID) dosimetry according to local practices. After reviewing the case, the physician asked for a rapid re-planning to reduce the absorbed dose to the teeth. A new treatment plan was created and approved. The operator initiated storage of the plan to the database ("Save all…"). In this case, the storage step involves the storage of three information objects in the following order: actual fluence, a digitally reconstructed radiograph (DRR), and the MLC control points (figure 2.1). A fundamental feature of database design is that if not all elements of a data object are successfully transferred (committed), an automatic roll-back to a previous consistent state of the database is initiated. Although the actual fluence was committed to the database, the DRR storage could not be completed owing to a "volume cache access" error. Therefore, the entire storage process was halted; an error message notified the user and asked whether the data should be saved before the application was aborted. By selecting the 'Yes' option, a second save process was initiated; however, it was unable to complete because the previous DRR transaction was still open and the software appeared to be frozen. Manual termination of the software (likely by 'ctrl-alt-del') caused a roll-back to the last consistent database state, which included the actual

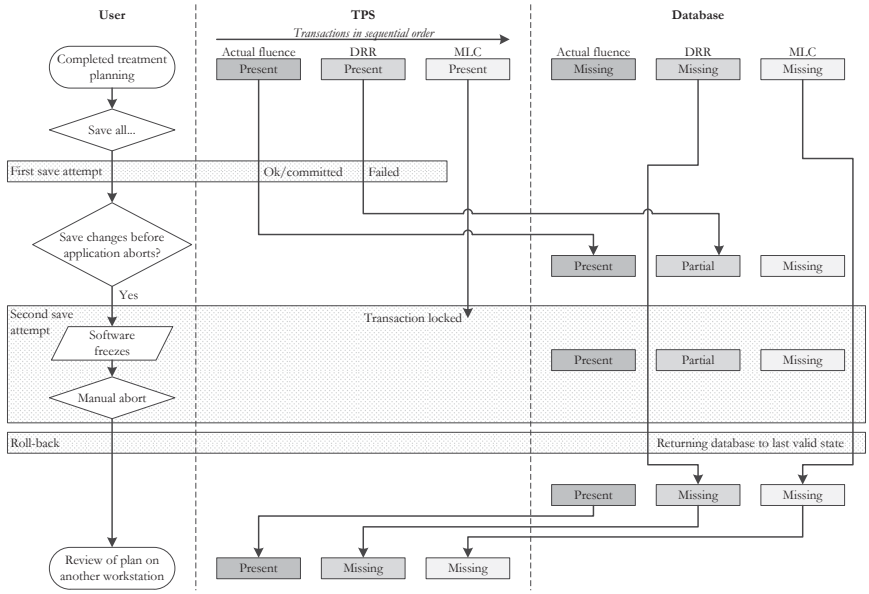

Figure 2.1. Flow chart illustrating the process of information storage from a user perspective and the corresponding system behaviour. Derived from the International Atomic Energy Agency (IAEA) training material.

fluence, but lacked the DDR and the MLC control point data. The plan was opened on another client, and the final dose distribution was calculated (which does not require the control point data). The missing MLC information was not detected, and the plan was approved for treatment. Because of the rush to start the patient on the new plan, no pre-treatment EPID dosimetry was performed until after three fractions had been delivered with the MLC fully retracted, at which point the fatal error was revealed.

(IAEA training material, New York State Department of Health 2005)

2.2 Manual transcription error

In January 2006, a 15-year-old patient received a 58% higher absorbed dose than intended during treatment of the central nervous system (CNS) at Beatson Oncology Centre in Glasgow. The cause of the accident was mainly related to procedural errors.

After an upgrade of the treatment management system (Varis, Varian Medical Systems), manual transfer of information between different modules was replaced by electronic transfer. However, for some of the most complex treatment plans (including the whole CNS treatment plan), the use of paper forms was retained. For these plans, the treatment parameters, including the number of MUs per fraction normalised to 1 Gy, were transferred to the treatment radiographer via a paper form. Several mistakes were made by the treatment planners involved in the planning process. The MUs were calculated for a fractionation schedule of 1.67×21 Gy, rather than for the prescribed absorbed dose of 1.75×20 Gy. However, the serious overexposure was not caused by the miscalculation, but by the failure to enter the MUs normalised to 1 Gy into the form. The radiographer calculated the MUs for input to the linear accelerator by multiplying the fraction absorbed dose of 1.75 Gy with the planned number of MUs, resulting in an actual fraction dose of 2.92 Gy. The mistake was not discovered until after 19 fractions had been delivered. At that point, another treatment planner observed the same planner making the same mistake again.

This complex treatment consisted of several groups of radiation beams. The beams delivered to the upper and lower spine were correctly calculated and administered. The head fields were delivered with 58% more MUs than intended. Thus, the 11×1.8-Gy targeted treatment for the tumour region in the head was abandoned after the CNS treatment. The patient died of recurrent pineoblastoma eight months after the accident.

(IAEA training material, Scottish ministers for the ionising radiation (medical exposures) regulations 2006)

2.3 Improper use of dynamic wedges

Many radiotherapy accidents have been reported in France in recent years, mainly because of the obligation to declare incidents related to the use of ionising radiation to the national safety authorities. The most severe accident affected 23 patients who received treatment for prostate cancer between May 2004 and August 2005 at Jean Monnet General Hospital in Épinal.

The treatment plans for these patients consisted of five 25 MV photon beams collimated with MLC. Four of these beams also had wedges in place. In May 2004, the hospital decided to change from static mechanical wedges (which were used prior to the accident) to dynamic wedges. However, some users continued to select the

mechanical wedge option in the TPS. The MUs (as calculated by the TPS) were manually transferred to the treatment unit and delivered using the dynamic wedge mode. The dynamic wedge required up to 50% fewer MUs than the static wedge to deliver similar absorbed dose distributions.

Unfortunately, the use of independent MU verification and *in vivo* dosimetry were abandoned at the same time that the dynamic wedges were introduced. Therefore, the errors were not detected, and 24 patients were overexposed by 20-35%. As a consequence of the accident, five patients died and at least ten patients have experienced severe complications.

(Derreumaux *et al.* 2008, General Inspectorate of Social Affairs 2007, IAEA training material)

2.4 Lessons learned

The accidents in New York and Glasgow highlighted the need for data transfer QA programs. Such QA programs should enable physicists to develop appropriate patient-specific QA procedures and tests for manually handled data (Siochi *et al.* 2011). Knowledge of information technology and standards for data exchange (e.g., the radiation therapy extension of DICOM, DICOM-RT) are essential in the design of these procedures, and an "under-the-hood" knowledge of the specific systems in the clinic is required in order to test treatment database integrity and assess whether related data are logically consistent with each other. By using *in vivo* dosimetry during the first fraction, all three errors could potentially have been detected and their consequences could have been reduced. However, the accident in New York highlighted the potential magnitude of errors during dynamic treatments. Instead of the intended 2 Gy fraction dose, 13 Gy were delivered with the MLC fully retracted. This result implies that *in vivo* dosimetry should preferably be evaluated in real-time to allow for early termination if errors are detected during treatment. If the measurements in New York had been completed and evaluated before the first treatment fraction, the error would have been detected before it was propagated to the patient. When introducing new technologies (e.g., dynamic wedges), a complete end-to-end test from CT scanning to treatment delivery might identify potential problems in the new clinical workflow. Independent MU verification based on the patient-specific machine parameters determined during the treatment planning process could potentially have prevented all of the accidents described above.

Relevant evaluation methods and action levels of the data acquired during the preventative QA activities described must be derived. Statistical process control (SPC) is commonly used when controlling manufacturing lines. SPC could provide relevant methods for monitoring the QA processes and determining statistically relevant action levels. When measurements are to be evaluated in real-time, the uncertainty in the time domain must be taken into account during the evaluation.

Section 4 of this thesis focuses on the development and evaluation of efficient tools that might prevent these types of accidents from recurring (and might also prevent many other types of accidents) if implemented in a clinical setting. The methods used for data analysis are described in Section 3. While the accidents described resulted in major radiation overdoses, the development of new tools within this thesis was also focused on the detection and prevention of smaller systematic and random errors.

3 The evaluation of measurements and calculation results

Data attributes were analysed in paper **I** to evaluate the data integrity between among DICOM-RT plan files. In paper **II**, SPC was used to analyse the difference in calculated absorbed dose between the TPS and an independent MU verification software developed within the framework of this thesis. In papers **III** and **IV**, the gamma evaluation method (Low *et al.* 1998) had a central role in comparisons between measurements and the TPS-calculated absorbed dose. The method was extended to incorporate an additional time-related dimension of the TPS-calculated data (**IV**). Percentage absorbed dose difference calculations (**II**-**V**) and isodose comparisons of 3D absorbed dose data (**V**) were also used in the evaluations. The developed extension of the gamma method as well as the principles of SPC are new evaluation concepts within the field of radiotherapy and are therefore further described in the following sections.

3.1 Statistical Process Control

Statistical process control (SPC) is the application of statistical techniques in order to monitor and improve processes. SPC allows for a quantifiable, numerical analysis of process variability with an emphasis on early detection and the prevention of problems.

Pawlicki *et al.* have provided some examples of SPC applications in radiotherapy QA (Pawlicki and Whitaker 2008, Pawlicki *et al.* 2005, Pawlicki *et al.* 2008b). The process of patient-specific IMRT QC measurement has been studied using SPC (Pawlicki *et al.* 2008), and SPC has also been proposed for monitoring the electron spectra from linear accelerators (de la Vega *et al.* 2012).

Unlike the classical approach of using the mean and standard deviation of the sampled data to characterise a process, SPC permits monitoring of the stability of process variability. The variation in data can be of two fundamentally different types. Common cause variations are random fluctuations that are expected to be present in

any set of measurements. Special cause variations arise from unpredictable, non-random events beyond the expected variability (Stapenhurst 2005). SPC analysis can be divided into understanding the process, determining the cause of its variability, and eliminating the source of special cause variations. To understand a process, it is usually mapped out and monitored using control charts.

Control charts is a key concept in SPC, and are used to distinguish between common and special cause variations. A point falling outside the control chart limits is an indication of a special cause variation. There are several different types of control charts available within SPC, and selecting an appropriate control chart can be a difficult task. Flow charts, based on the data to be plotted and the format in which the data are collected, can aid this decision (figure 3.1).

The Shewhart individuals control chart (individual/moving range chart, or XmR chart) had a central role in paper **II**. The data in this paper were chronologically organised individual calculation results, and the XmR chart was therefore used. The XmR chart concept contains two types of charts: one that displays the individual measured values (X chart), and one that displays the difference from one measurement to the next (mR chart).

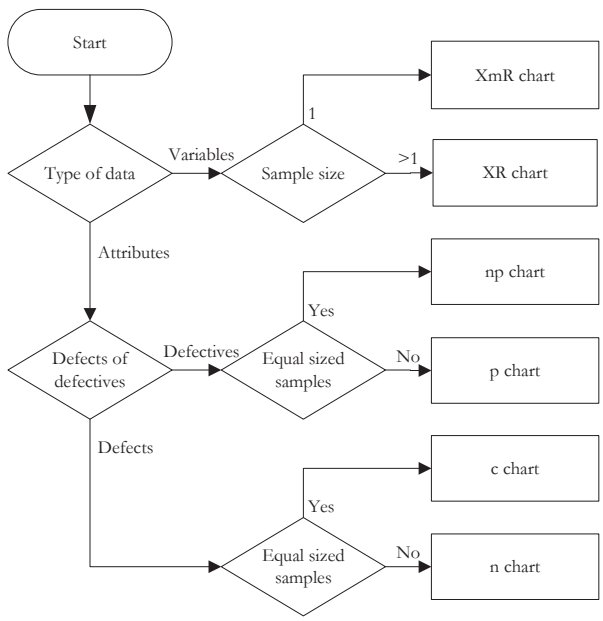

Figure 3.1. Example of a flow chart for selecting an appropriate control chart.

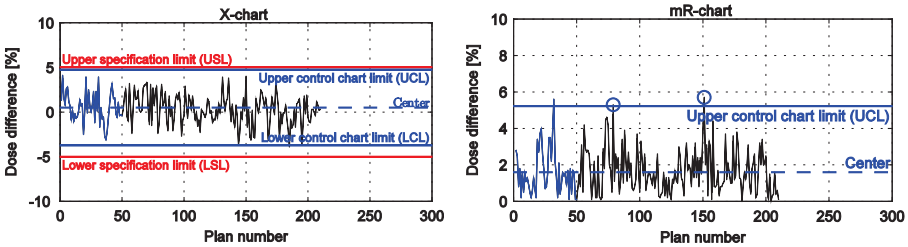

Figure 3.2. Control charts for one of the processes analysed in paper **II** (head-and-neck at Institution 2). The blue data points (first 50) were used to calculate the upper and lower control chart limits (blue lines). The blue circles represent data points that fall outside the control chart limits, and therefore indicate potential special cause variations.

Figure 3.2 illustrates the concept of the XmR chart. In this case, each point represents a dose difference calculation between TPS and the independent MU verification software.

The moving range (mR_i) is determined by equation (3.1), where x_i represents a single measurement. $\overline{mR}$ is the average moving range between successive data points (3.2) and hence a measure of the dispersion of the data. This constitutes the centre line of the mR chart. The number of dose difference calculations is denoted n.

$$mr_i = \left| x_i - x_{i\text{-}1} \right| \tag{3.1}$$

$$\overline{mR} = \frac{\sum_{i=2}^{n} mR_i}{n-1} \tag{3.2}$$

The upper control chart limit (UCL) for the mR chart is calculated using:

$$UCL = D_4 \cdot \overline{mR} \tag{3.3}$$

Upper and lower control chart limits for the X charts are calculated using equations (3.4) and (3.5), where $\overline{x}$ is the average of all individual measurements.

$$UCL = \overline{x} + \frac{3 \cdot \overline{mR}}{D_2} \tag{3.4}$$

$$LCL = \overline{x} - \frac{3 \cdot \overline{mR}}{D_2} \tag{3.5}$$

The constants D2 and D4 are sample size dependent anti-biasing constants, the values of which are available in textbooks (Montgomery 1996). The constant 3 has traditionally been used as a trade-off between the sensitivity of the control chart and the resources available to determine the cause of data points falling outside the limits (Shewhart 1931). As a rule of thumb, 25 data points have been recommended as a minimum for the calculation of control chart limits (Shewhart 1931). Using a small number of initial data points to calculate the limits could be beneficial for processes with low throughput (otherwise, it would take a long time before they could be monitored). However, the uncertainty in the computed limits will decrease as the amount of data used to compute the limits increases.

Process capability analysis can be performed to determine a process' ability to generate results within specification. The process capability index determines whether a process is able to meet its specification. The specification limit is a statement of the user requirement, and has no connection to the control chart limit, which is estimated from the data. For normally-distributed data, the capability index is calculated as:

$$\hat{C}_{pk} = min\left[\frac{USL - \overline{x}}{3s}, \frac{\overline{x} - LSL}{3s}\right] \tag{3.6}$$

USL and *LSL* are the upper and lower specification limits, respectively. $\overline{x}$ and *s* are estimates of the mean and the standard deviation of the process, respectively.

3.2 Gamma evaluation

The gamma evaluation method (Low *et al.* 1998) has been widely accepted for comparisons between two dose distributions in 1-3 dimensions. It combines the distance to agreement and the dose difference into a single measure. For a dose profile (1-dimensional dose distribution, $\vec{r} \in \mathbb{R}^1$), the two criteria can be visualised as an ellipse in which the boundary represents the acceptance criterion (figure 3.3, left). The equation of the ellipse can be written as:

$$1 = \sqrt{\frac{r^2\left(\vec{r}_m, \vec{r}\right)}{\Delta d^2} + \frac{\delta^2\left(\vec{r}_m, \vec{r}\right)}{\Delta D^2}} \tag{3.7}$$

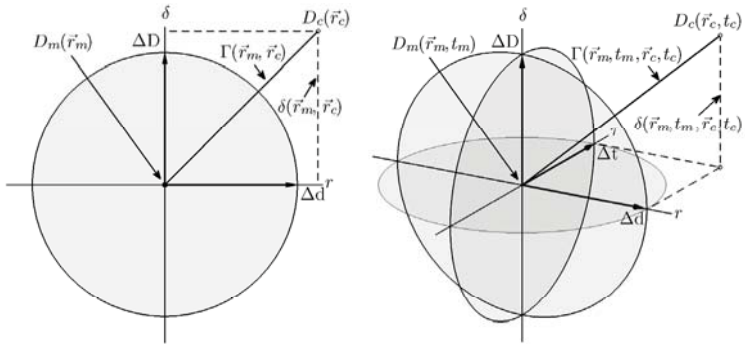

Figure 3.3. A graphical representation of the traditional (left) and extended (right) gamma evaluation methods.

The gamma index is defined as:

$$\gamma_H\left(\vec{r}_m\right) = \min\left\{\Gamma_H\left(\vec{r}_m, \vec{r}_c\right)\right\} \forall \left(\vec{r}_c\right), \tag{3.8}$$

where

$$\Gamma_H\left(\vec{r}_m, \vec{r}_c\right) = \sqrt{\frac{r^2\left(\vec{r}_m, \vec{r}_c\right)}{\Delta d^2} + \frac{\delta^2\left(\vec{r}_m, \vec{r}_c\right)}{\Delta D^2}} \tag{3.9}$$

A point $\vec{r}_c$ inside the ellipse will have $\Gamma_H\left(\vec{r}_m, \vec{r}_c\right) < 1$, and the gamma evaluation passes thereby the test at $\vec{r}_m$.

When evaluating measurements as a function of time, uncertainties in the time domain will greatly influence the result. Therefore, the gamma evaluation method was extended to incorporate a criterion related to time difference (**IV**). For rotational treatments (e.g., VMAT), the gantry angle is a function of time; therefore, it is practical to use the gantry angle instead of time as the time-related criterion (Δt). The extended method simultaneously takes the dose difference, the distance in the Cartesian space, and the time difference into account (figure 3.3, right).

All points $\left(\vec{r}_m, t_m\right)$ are evaluated, where $\vec{r}$ represents the spatial localisation in 1-3 dimensions and t represents a position in the time domain. For comparisons between measurements and calculations, the first axis (r) is the Euclidean distance between the measurement point and the calculation point, the second axis (τ) is the time difference, and the third axis is the dose difference (D) between the measured absorbed dose [$D\left(\vec{r}_m, t_m\right)$] and the calculated absorbed dose [$D\left(\vec{r}_c, t_c\right)$]. The surface of the ellipsoid that defines the acceptance criterion is now defined as:

$$1=\sqrt{\frac{\tau^2(t_m,t)}{\Delta t^2}+\frac{r^2(\vec{r}_m,\vec{r})}{\Delta d^2}+\frac{\delta^2(\vec{r}_m,t_m,\vec{r},t)}{\Delta D^2}}, \tag{3.10}$$

where

$$\tau\left(t_m,t\right)=t-t_m, \tag{3.11}$$

$$r\left(\vec{r}_m,\vec{r}\right)=\left|\vec{r}-\vec{r}_m\right|, \tag{3.12}$$

and

$$\delta\left(\vec{r}_m,t_m,\vec{r},t\right)=\delta\left(\vec{r},t\right)-\delta\left(\vec{r}_m,t_m\right) \tag{3.13}$$

If any part of the surface $D\left(\vec{r}_c,t_c\right)$ intersects the ellipsoid, the test passes the criterion at $\left(\vec{r}_m,t_m\right)$. When $\vec{r}\in\mathbb{R}^n$, $n\geq 2$ and all criteria have the same numerical value, the surface defined by the acceptance criteria will constitute a hypersphere (3-sphere or 4-sphere). The hyper-gamma (γ_H) can now be defined as:

$$\gamma_H\left(\vec{r}_m,t_m\right)=\min\left\{\Gamma_H\left(\vec{r}_m,t_m,\vec{r}_c,t_c\right)\right\}\forall\left(\vec{r}_c,t_c\right), \tag{3.14}$$

where

$$\Gamma_H\left(\vec{r}_m,t_m,\vec{r}_c,t_c\right)=\sqrt{\frac{\tau^2\left(t_m,t_c\right)}{\Delta t^2}+\frac{r^2\left(\vec{r}_m,\vec{r}_c\right)}{\Delta d^2}+\frac{\delta^2\left(\vec{r}_m,t_m,\vec{r}_c,t_c\right)}{\Delta D^2}} \tag{3.15}$$

As in the original gamma evaluation method, the evaluated point passes the test if $\gamma\leq 1$. The ratio between the number of sampling points with $\gamma\leq 1$ and the total number of points is referred to as the gamma pass rate.

4 Quality Assurance

A comprehensive QA program includes all aspects of patient care (e.g., physical, clinical, and medical aspects) (Saw *et al.* 2008). This chapter focuses on the physical aspects of the radiotherapy process that were prioritised within the framework of this thesis.

4.1 Transfer of information

To allow different medical systems to communicate with each other, a global information technology standard has been developed: Digital Imaging and Communications in Medicine (DICOM) (NEMA 2011). Today, DICOM encompasses both communication protocols and file formats, allowing it to act as a base for the intersystem transfer of digital medical images. The standard has also been extended for use in other specialties. One of the first extensions was applied to radiation therapy, and is known as DICOM-RT (Law and Liu 2009). DICOM-RT is an integral part of the Integrating the Healthcare Enterprise in Radiation Oncology (IHE-RO) initiative, which aims to help users and vendors to develop approaches for integrating various radiation oncology systems (Abdel-Wahab *et al.* 2010). Today, DICOM-RT is a widely accepted information-technology standard and has a major role in the communication between different systems used in the radiotherapy process. The absence of manual data transfer improves data integrity (Clark *et al.* 2010). However, manual data input might be difficult to avoid at some steps of the treatment chain, which inevitably leads to an increased risk of errors (Cunningham *et al.* 2010, Holmberg and McClean 2002).

As the complexity of radiation treatment increases, so does that of the software used in the radiotherapy process. Although some systems are developed to suit a specific isolated task, more often systems are able to perform different tasks and the functionalities of different systems in the radiotherapy environment tend to overlap. The user is able to edit data and add complementary information in several of these systems. The relevance and consistency of these data changes are not always clear to

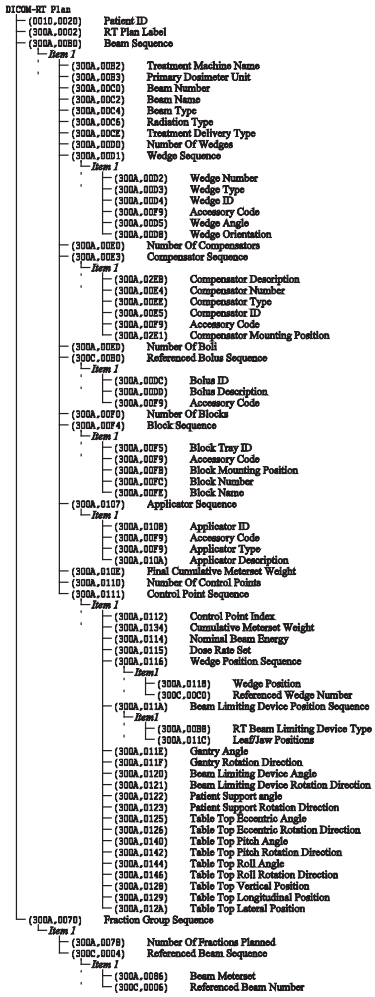

Figure 4.1. The hierarchy of DICOM attributes used in the integrity check.

the individual user, which may result in unwanted consequences (Leunens *et al.* 1992). New tools are needed to manage data integrity issues in radiotherapy (Knöös *et al.* 2001). The development and evaluation of such tools, based on the DICOM standard, was the aim of paper **I**. These tools could be used as an integral part of many QA processes that have been designed based on the checklist provided in a rapid communication on external beam radiotherapy data transfer authored by American Association of Physicists in Medicine (AAPM) Task Group 201 (Siochi *et al.* 2011).

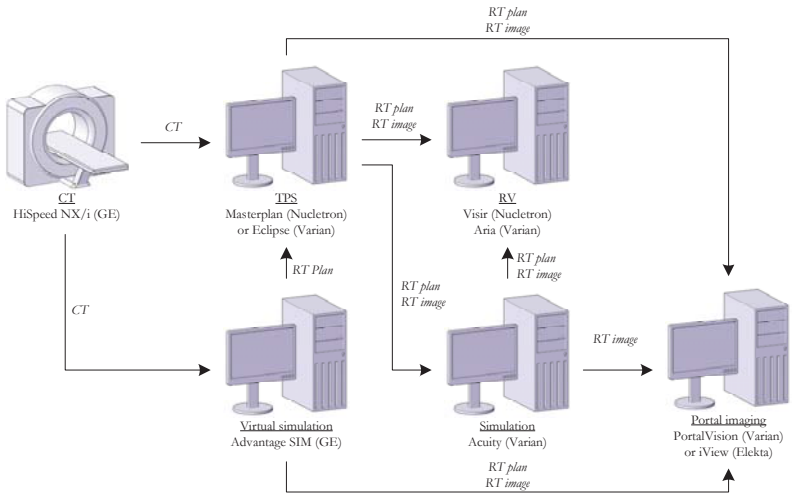

Figure 4.2. The transfer of DICOM information in the clinical environment.

A general DICOM-RT plan comparison method for ensuring the integrity between any two DICOM-compatible systems was developed using the MATLAB (MathWorks inc.) environment. The DICOM attributes that are directly related to the treatment unit setting and identification of treatment devices (e.g., blocks, boli) were identified from the DICOM standard. All DICOM attributes considered in the plan comparison are shown in figure 4.1, which also illustrates the hierarchy of the data. The developed software was used to compare three different combinations of TPS and record-and-verify systems with respect to data integrity in a clinical multi-vendor environment (figure 4.2).

The data integrity analysis was divided into two steps. In the first step, all parameters were compared without any tolerance level, and a normal condition for each system combination was identified. The normal condition constitutes clinically accepted systematic data alterations arising from software designs and/or clinical procedures. The number of deviations in this step of the analysis normalised to the total number of beams was used as a measure of the level of integrity for the system combination. The system combination with the highest level of data integrity was the Eclipse→Aria combination, which shares a single database (table 4.1).

In the second step, parameters were excluded if their associated DICOM attributes were missing from one or both systems. Tolerances were used to manage the rounding of decimal values to isolate potential special cause deviations outside the normal conditions, and lookup tables were used for data that are mapped in the import and/or export in the systems. Only MLC positions for leaves defining the beam aperture shape were compared for the Masterplan→Visir combination, because

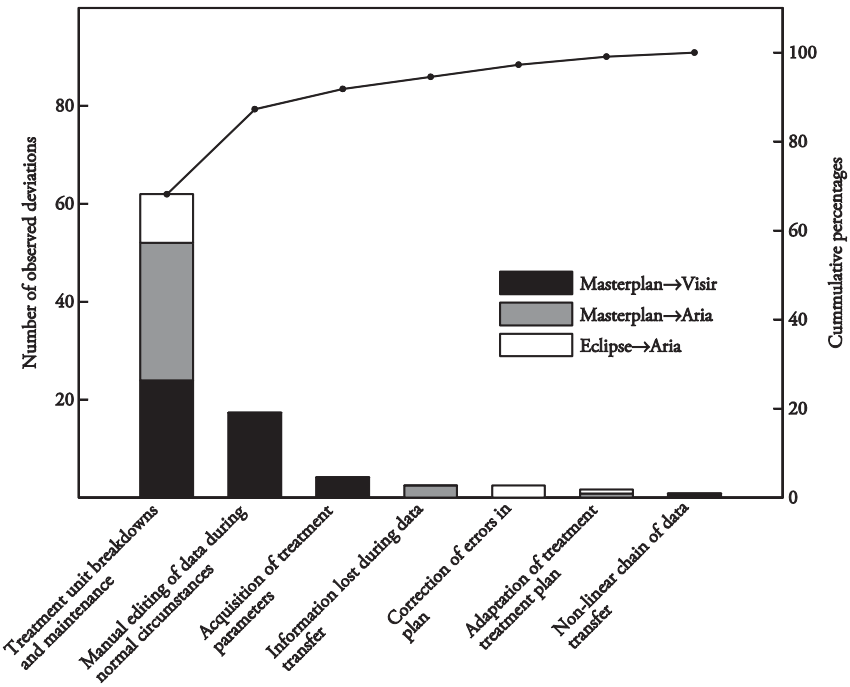

Figure 4.3. Number of plans with discrepancies per category, identified in the second step of the analysis. 100 plans were analysed for each system combination.

Visir does not export MLC positions outside the beam opening (i.e., MLC positions set to zero).

The discrepancies from the second step of the analysis were classified into seven different categories based on how they occurred (figure 4.3). Only two types of discrepancies were observed for more than one system combination: treatment unit breakdowns and maintenance, which affected the number of fractions planned, and adaptation of treatment, which affected collimator positions and meter sets. None of

Table 4.1. Number of discrepancies per beam, identified in the first step of the analysis.

Treatment planning system	Record-and-verify system	Number of discrepancies
Masterplan (Nucletron)	Visir (Nucletron)	10.9 per beam
Masterplan (Nucletron)	Aria (Varian)	4.9 per beam
Eclipse (Varian)	Aria (Varian)	3.1 per beam

these discrepancies arose in the physical transmission of the data (e.g., due to network failures); rather, they were related to clinical procedures and system designs. If dosimetrically matched treatment units had been available, integrity issues associated with treatment re-planning could have been avoided by allowing the same plan to be treated at another unit.

The proposed method can constitute an important part of a data QA program by allowing patient-specific data to be monitored and potential compatibility problems between different radiotherapy systems to be identified. Logical consistency testing (e.g., IMRT treatment plans must have an MLC) can also be implemented in the software, which could prevent accidents such as the one that occurred at St. Vincent's Hospital.

4.2 Independent monitor unit verification

MU verification is a central part of the patient-specific QA process (Nyholm 2008, Sellakumar *et al.* 2011). Many radiotherapy accidents, such as the ones that occurred at Beatson Oncology Centre and Jean Monnet General Hospital, might have been prevented if a secondary independent MU control system had been used routinely (Stern *et al.* 2011). Ideally, independent refers to the data used to characterise the treatment unit, the implementation of the calculation algorithms, and the derivation of geometrical data (e.g., source-to-surface distance, depth, and radiological path length) from the patient anatomy. Using shared input data will increase the risk of errors that affect both systems, and therefore would be difficult to detect.

Several calculation methods have been proposed for the purpose of MU verification, ranging from factor-based models to Monte Carlo simulations (Dutreix *et al.* 1997, Kung *et al.* 2000, Nyholm *et al.* 2006, Pisaturo *et al.* 2009).

MU verification software was developed within the framework of this thesis (Radiotherapy Verification Program, RVP) based on two factor-based models. The first method incorporates an expression for the linear attenuation of the primary photons and an expression for the ratio of scatter photons to primary photons (scatter-to-primary ratio, or SPR). The second method is based on percentage depth dose tables and output ratios in water for different field sizes and a single reference source-to-surface distance (SSD). Heterogeneities inside the patient are taken into account by manually entering the length of bulk density tissues along the beam path to the calculation point. The RVP software has been adopted at several Swedish institutions for pre-treatment verification of 3D-CRT treatments. This has allowed

detailed statistical analyses analysis of the MU verification process based on a large collection of data (**II**).

An essential part of the MU verification process is the definition of relevant action levels for deviations between the primary and secondary calculations. The accuracy of the two calculation methods in clinically relevant situations forms the basis for these action levels (Stern *et al.* 2011). The statistical analyses were therefore based on the tools within SPC. Deviations between point dose calculations in TPS and in RVP for 9219 treatment plans from five different institutions were analysed using control charts. Based on previous experience with the SPR calculation model (Knöös *et al.* 2001), a ±4% action level was used at all institutions during the data collection period. The process of MU verification was divided into subprocesses based on the stored treatment plan parameters (e.g., institution, treatment unit, treatment site, signature/operator, and number of beams). Differentiation into institutions, treatment sites, and treatment techniques derived the most meaningful subprocesses for the purpose of generating control charts. Although only data from RVP were analysed in this study, the concept of control charts and subprocesses might also be valid for other MU verification software.

For the subprocesses, centre line values ranged from -1.7% to 1.6%, and the half widths of the limits ranged from 1.8% to 6.8%. The half widths of the limits were in good agreement with the guidelines for action levels proposed by AAPM Task Group 114 regarding the verification of MU calculations (Stern *et al.* 2011). Therefore, control charts may provide an efficient means of deriving action levels for use in conjunction with the recommendations of Task Group 114. However, the use of control charts should not replace a comprehensive commissioning of either the MU verification software or the primary TPS.

Nineteen of 32 subprocesses met the clinical specification (±5%) (i.e., capability index ≥1). The specification level of 5% absorbed dose difference was chosen after considering the combined uncertainty between RVP and TPS, as well as the overall accuracy requirements of 2.5-3.5% (1 s.d.).

The total percentage of calculations outside the control chart limits was 2.1% for the subprocesses analysed, and major differences (0.0–10.3%) between subprocesses were identified. The major differences originated from the categorisation of treatment plans. The subprocess for which many calculations fell outside the limits was characterised by a small half width between the limits, due to very similar patient geometries and beam settings. However, the data also contained a few plans associated with a completely different beam setting and geometry, which therefore had a high

likelihood of falling outside the limits. These plans should have been placed in another subprocess.

Differences in control chart parameters for investigated subprocesses were observed between different treatment sites, treatment techniques, institutions, and users.

The differences between different treatment sites and techniques were mainly caused by various degrees of complexity. For more complex treatments (e.g., treatment of the breast using asymmetric technique), the corresponding capability was low because of limitations in the factor-based models. Subprocesses for which it is possible to select the calculation point such that that it fulfils the recommendations of the International Commission on Radiation Units and Measurements for prescribing and reporting absorbed dose (i.e., points where transient electron equilibrium is established) result in a smaller width between the control chart limits and a higher process capability.

For treatment sites associated with heterogeneous volumes, institutions with higher moving range and lower process capabilities also exhibited larger variation between users (i.e., signatures). Some users also exhibited a larger variation in their calculation results compared with their institution colleagues. This finding indicates that the difference did not arise from the beam data in TPS or RVP, but from how stringent the methodology for MU verification was at that institution. By reducing the flexibility in the software (e.g., by introducing non-user-associated determination of geometrical parameters and the use of a well-defined methodology for the process), these user variations could be minimised.

The data is analysed chronologically using control charts, which enables early detection of changes in a process. At one institution, a migration from using the pencil beam convolution (PBC) algorithm in MasterPlan to the anisotropic analytical algorithm (AAA) in Eclipse was undertaken during the data collection period. The effect of this change can be seen as an increase in the mean value after 156 calculated plans, while the average moving range remains at a similar level (figure 4.4). Having implemented SPC, the points outside the control chart limits would have triggered an investigation and potentially revealed the effect of the migration to AAA and Eclipse on the process of MU verification. After determining and accepting the cause of the change in the process, the modified process should be mapped out and new control chart limits should be calculated.

It was concluded that the construction and analysis of the control charts can improve the understanding of the MU verification process from a clinical point of view, and can also allow for statistically relevant treatment sites and technique-specific action levels (control chart limits) to be applied. The control chart is also a valuable tool

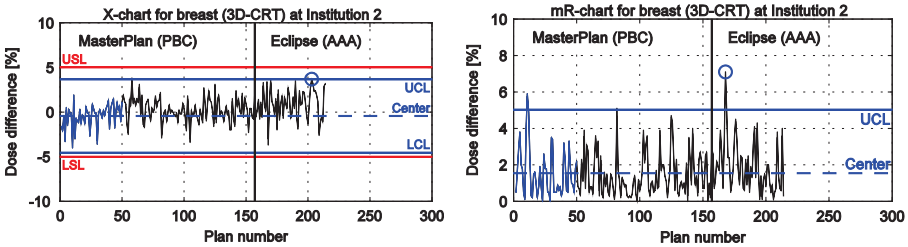

Figure 4.4. Control charts for the subprocess derived from the breast treatment site and 3D-CRT treatment technique at a single treatment unit. The PBC algorithm in MasterPlan was used until calculation 157, when the AAA algorithm in Eclipse was implemented. The blue data points represent the initial 50 plans used to determine the control chart limits. The red lines represent the specification level of ±5%.

with which to identify systematic errors and weaknesses in radiotherapy-related processes.

4.3 Pre-treatment measurements

Since the introduction of IMRT, pre-treatment measurements have been widely employed as a part of routine patient-specific QC of intensity-modulated treatments. Film dosimetry has gradually been replaced by different types of detector arrays (Buonamici *et al.* 2007). As VMAT has found its way into clinical practice, so have new detectors and plan verification methods.

VMAT plans are often highly modulated and contain many degrees of freedom: the dose rate, gantry speed and MLC positions are all simultaneously variable (Korreman *et al.* 2009). The QA of VMAT plans is generally derived from (or similar to) that of IMRT. This includes the use of diode or ionisation chamber arrays, or portal dosimetry systems. Recently, new diode arrays that may be well suited for rotational measurements have been developed, such as the Delta^4 (Scandidos) and the ArcCheck (Sun Nuclear) (Bedford *et al.* 2009, Feygelman *et al.* 2011, Petoukhova *et al.* 2011).

Because VMAT plan delivery involves continuous gantry movement, rather than a discrete number of gantry angles, there are usually no patient plan-specific control measurements of anything other than the entire composite dose distribution. It is possible that some deviations between planned and delivered dose distributions at

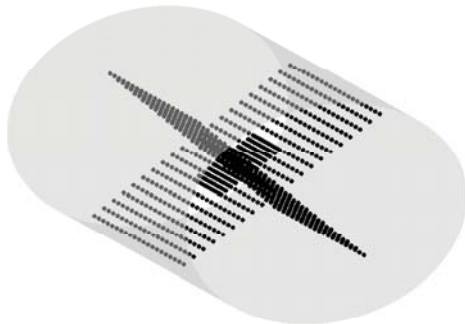

Figure 4.5. Illustration of the Delta[4] detector system, which consists of two orthogonal detector arrays in a cylindrical polymethyl methacrylate (PMMA) phantom. The detector spacing is 5 mm in the central and 10 mm in the distal part of each array.

certain gantry angles cancel each other out when only the composite dose distribution is analysed. In turn, potential delivery errors are blurred, and information regarding how well the accelerator is coping with the delivery of these types of complex plans can be lost. Each VMAT beam is described by a number of control points. By analysing VMAT delivery at a control point level, both systematic and plan-specific errors that are not visible in the composite plan could potentially be found.

To evaluate the accuracy of the AAA algorithm in the Eclipse treatment planning and the delivery system (Clinac iX, Varian Medical Systems), measurements of VMAT plans were compared with the corresponding treatment plans at a control point level (**III**). For this purpose, clinical treatment plans of varying complexity were analysed using the Delta[4] detector system (figure 4.5).

Ten treatment plans with principally different properties (e.g., target size, number of arcs, photon energy, and number of MUs) were included in this retrospective study. Each plan was measured five times during a 7-day period using a research version of the Delta[4] software. This version allowed the dosimetry readings, acquired at 72 Hz, to be exported and analysed using an application software developed in-house with support for 4D TPS dose distributions and hyper-gamma functionality. The measurements were analysed control point by control point using the developed hyper-gamma method and the [2%/2mm/0.5°] and [3%/3mm/0.5°] criteria.

Table 4.2. Uncertainties associated with the gantry angle determination for two full arcs of different rotation directions (1 s.d.).

Arc	Inclinometer mounting position	N62u	IK360	DynaLog
1-2	Plastic cover	0.64°	0.74°	0.087°
3-4	Metal frame behind cover	0.20°	0.13°	0.083°

For VMAT treatments, the gantry angle is directly related to a specific control point. To group the dosimetry readings into control points, different methods were investigated to acquire the gantry angle at the time of the dosimetry reading. The uncertainties in the gantry angle determination were evaluated for two different inclinometers: N62u (Nordic Transducer) and IK360 (SIKO). Different mounting positions, as well as the uncertainties associated with the MLC computer-generated DynaLog files (VMS 2011), were examined (table 4.2). If inclinometers are used for precision gantry angle measurements, they should not be mounted on the plastic cover. The reason for this is that small movements of the covers are present at certain angles. The DynaLog files were associated with the least uncertainty, and were therefore used to group the dosimetry data. However, the DynaLog data are not independent of the accelerator; therefore, simultaneous IK360 measurements were used to verify the actual gantry angle readings.

To allow efficient evaluations of the large data collections acquired, the data were collapsed into a 2D view by displaying the hyper-gamma pass rates for the two detector planes side by side. This allowed spatial areas with potential issues to be identified. Profile comparisons in the spatial and control point intervals dimension were used to identify specific control point intervals for further investigations using beams-eye-views (figure 4.6). The beams-eye-view was found to be a valuable tool in the determination of the cause of e.g. low hyper-gamma pass rates for specific gantry angle intervals and detector elements.

From the hyper-gamma analyses, it was concluded that the AAA and Clinac iX delivery system were accurate within small control point intervals, for both 6 MV and 10 MV. The average hyper-gamma pass rates [3%/3 mm/0.5°] were above 93% for all plans investigated. There was a concern that gravitational effects could affect the MLC and hence the accuracy in specific gantry angle intervals. However, no significant difference between different gantry angle intervals were observed, except for those associated with the two first and last control points for a 358° arc. It is unlikely that this discrepancy would have any clinical impact, since it constitutes a very small part of the total treatment.

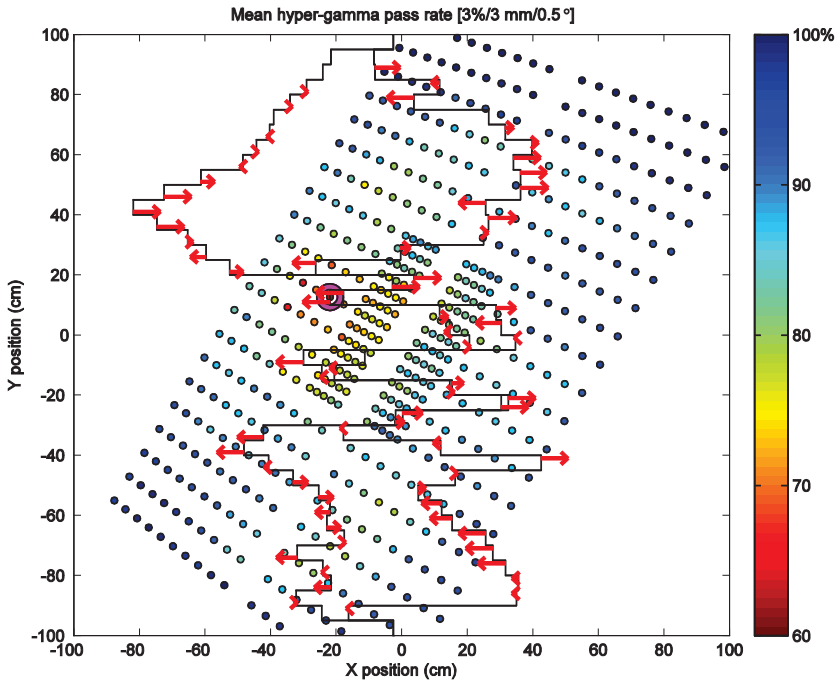

Figure 4.6. The mean hyper-gamma pass rates for the wing units of the Delta[4] detector system and a single arc displayed in beams-eye-view. The red arrows illustrate the motion of the individual MLC leaves from the start to the end of the control point interval. A small MLC opening moving rapidly over one detector element (purple circle) was discovered. This caused a large absorbed dose difference between calculation and measurements for this particular detector element and control point interval.

4.4 *In vivo* dosimetry

In vivo dosimetry is the most direct method for monitoring the absorbed dose delivered to the patient. Unlike other QA procedures, *in vivo* dosimetry checks the absorbed dose delivered to the patient rather than the individual components prior to treatment (AAPM 2005, Essers and Mijnheer 1999). Errors occurring at the time of treatment would not be detected with pre-treatment measurements, although they might be detected through the use of *in vivo* dosimetry. *In vivo* dosimetry is an important safeguard against major treatment delivery errors in external beam

radiotherapy (Calandrino *et al.* 1997, Cunningham *et al.* 2010, Essers and Mijnheer 1999, Fiorino *et al.* 2000, Lanson *et al.* 1999, Noel *et al.* 1995). The investigations of the accidents at Beatson Oncology Centre and Jean Monnet General Hospital concluded that they could have been prevented by the use of *in vivo* dosimetry during the first treatment fraction. The accident at St. Vincent's hospital highlighted the potential magnitude of errors during dynamic treatments. The potential magnitude implies that *in vivo* dosimetry should preferably be evaluated in real-time to allow for early termination if errors are detected during treatment.

Despite the many examples of accidents that could have been prevented by the use of *in vivo* dosimetry, the cost versus the benefit of *in vivo* dosimetry has been argued and the scientific community has not reached a consensus (MacKay and Williams 2009, McKenzie *et al.* 2006, Williams and McKenzie 2008). For IMRT, *in vivo* dosimetry using EPIDs may constitute an efficient system (McDermott *et al.* 2007). The additional clinical time required for *in vivo* EPID dosimetry is small, because the detector does not need to be attached to the patient and the reading is acquired during treatment. However, the dose reconstruction time is a limiting factor for real-time *in vivo* usage.

During recent years, electromagnetic (EM) transponder systems have been introduced to monitor intrafractional target motion (Cherpak *et al.* 2009, Kindblom *et al.* 2009, Shah *et al.* 2011). An advantage of EM localisation systems compared with most other localisation techniques is that they provide real-time positional information without the delivery of ionising radiation. By including a small radiation dosimeter in these types of devices, target absorbed dose can potentially be monitored *in vivo* with little extra effort. A complete evaluation system for real-time *in vivo* dosimetry was developed around the RayPilot (MicroPos) localisation system and evaluated using an anthropomorphic phantom (**IV**).

The RayPilot system consists of three parts: a transmitter, a receiver unit placed on the treatment couch, and a computer for real-time data analysis (i.e., determination of transmitter position). When used clinically, the wired transmitting probe is temporarily inserted into the prostate gland through perineal implantation, using a modified Seldinger technique. A p-i-n diode dosimeter was incorporated inside the probe near the transmitter, allowing simultaneous absorbed dose measurements and position monitoring in three dimensions.

An open water container was integrated with the anthropomorphic phantom to allow generation of intrafractional motion using a programmable 3D motion stage. The entire *in vivo* dosimetry system and the experimental setup are illustrated in figure 4.7.

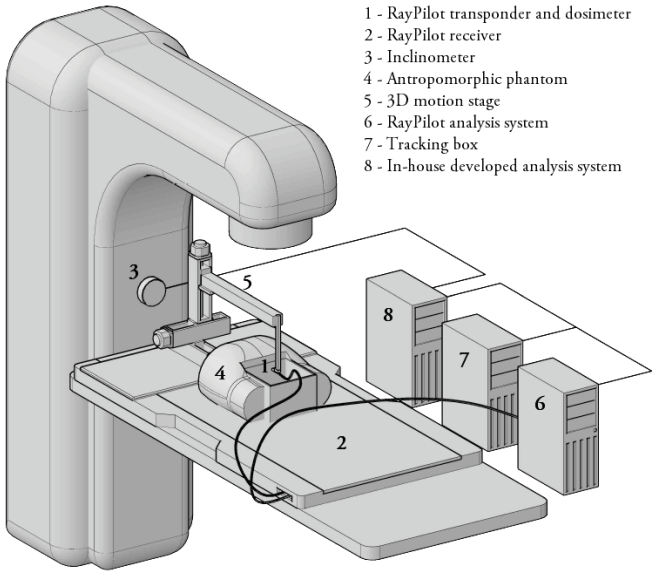

Figure 4.7. The experimental setup. The tracking box was only used to record readouts from the linear accelerator (e.g. gantry angle) synchronously with the RayPilot data.

To evaluate the proposed method for real-time *in vivo* dosimetry, errors were intentionally introduced into a typical 6 MV prostate VMAT plan. The plan was delivered using a Trilogy linear accelerator (Varian Medical Systems) both with and without intrafractional motion, and with and without errors introduced. Ideally, the *in vivo* dosimetry system should be able to distinguish the plans with introduced errors from the error-free plan. This methodology has previously been used to evaluate different detector systems (Damkjær 2011), and has also been proposed for the determination of acceptance criteria for measurements of IMRT plans (Carver *et al.* 2011). The errors introduced were:

- MUs increased by 3% and 5%
- Collimator rotation offset by ±3° and ±5°
- Both MLC banks shifted by ±3 mm and ±5 mm
- MLC opening increased by 1 mm and 3 mm
- MLC opening reduced by 1 mm and 3 mm, with a minimum opening of 0.6 mm.
- Gantry angle offset by ±3° and ±5°
- MLC fully retracted

All deliveries were evaluated using the hyper-gamma method and the [3%/3mm/1°] criteria, as well as the cumulative absorbed dose difference.

Reference absorbed dose data was extracted from the clinical TPS at every control point throughout delivery. The gantry angle was measured using a high-performance inclinometer (N62u, Nordic Transducer) and used to determine the current treatment progress (regarding the control point reached) and, in turn, the corresponding TPS-calculated absorbed dose.

The maximum difference between all dosimeter readings and the corresponding TPS-calculated cumulative absorbed doses for three consecutive deliveries with a static detector position and without introduced errors ranged from -3.7% to -2.3% of the total TPS-calculated absorbed dose. The hyper-gamma pass rate ranged from 95% to 100% for these deliveries.

The introduction of intrafractional motion had a substantial impact on the measured absorbed dose for two of the trajectories investigated. Determination of the reference TPS-calculated absorbed dose based on the EM-recorded positions generally reduced the deviations between the measurements and calculations. By comparing these values with non-positional corrected reference doses, the dosimetric effect of intrafractional motion could be estimated, and potential delivery errors could be isolated.

The absorbed dose difference exceeded the maximum absolute difference of the non-erroneous deliveries (3.7%) for three of the introduced errors and all trajectories. These errors were a 5% increase of MUs, MLC opening reduced by 3 mm, and a fully retracted MLC. The most severe treatment error (fully retracted MLC) was detected during an early stage of treatment (figure 4.8). Serious radiation overexposure can be avoided in a clinical setting by allowing the *in vivo* system to interrupt treatment if the measurements are outside pre-defined tolerance levels.

It was found that if implantable EM-transponders are used for target localisation, the addition of a dosimeter and an online dosimetric evaluation system provides a fast and resource-efficient *in vivo* dosimetry system. Combining the analyses of absorbed dose differences with hyper-gamma analyses allows for the detection of small treatment errors, as well as the evaluation of the dosimetric impact of intrafractional motion.

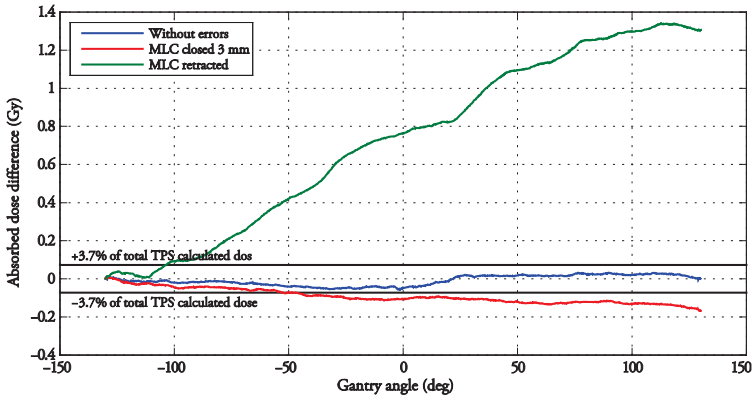

Figure 4.8. Plans delivered with high frequency oscillation trajectory.

4.5 End-to-end tests

When new technologies and methods are introduced, the need for verification of the entire treatment process is imminent. Polymer gel dosimetry can be used to measure absorbed dose distributions in a complete volume with high spatial resolution (Isbakan *et al.* 2007, Vergote *et al.* 2004). By substituting a gel dosimetry phantom for the patient, the radiotherapy process from CT-scanning to treatment delivery (including treatment planning and patient setup strategies) can be checked. The gel dosimeter can either function as the phantom itself or as a part of the phantom. The measured dose can be compared with the TPS-calculated dose distribution, evaluating both the dosimetric and geometric accuracy of the treatment.

Polymer gel dosimetry involves three steps: fabrication, irradiation, and scanning (Baldock *et al.* 2010). Owing to the introduction of oxygen scavengers, the dosimeters can be fabricated at normal room atmosphere (Fong *et al.* 2001). The polymer gel mainly consists of ultra-pure deionised water (approximately 90%) and is therefore equivalent to soft tissue (Keall and Baldock 1999). The other components include radiation-sensitive chemicals (monomers) and a matrix substance (e.g., galatine). A process of radiolysis starts when the gel is irradiated; highly reactive radicals induce the monomers to form polymers. The amount of polymer produced depends on the absorbed dose deposited in the volume. The role of the gel matrix is to preserve the spatial integrity of the polymer structures.

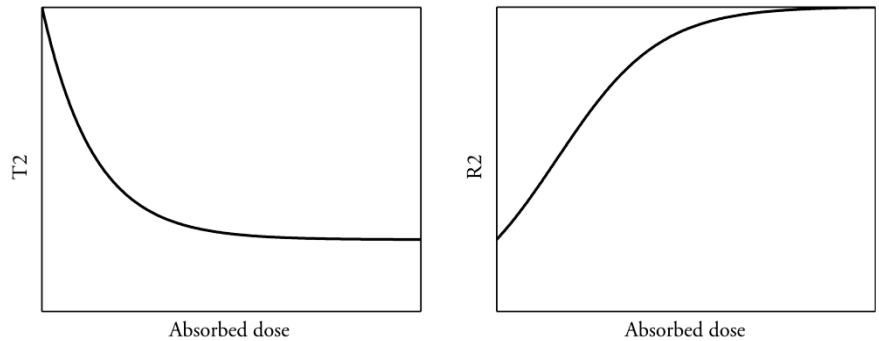

Figure 4.9. Illustration of the relationship between T2, R2 and the absorbed dose for polymer gel dosimeters.

The absorbed dose information can be read out using different imaging techniques (e.g., MRI, optical-CT and x-ray CT). The parameter that is most commonly used to determine the absorbed dose is the relaxation rate of transversal magnetisation (*R2=1/T2*) (Baldock *et al.* 2010). This parameter can be determined by MRI using multiple spin echo sequences. The *R2* increases with increased absorbed dose, and is approximately linear within a limited range (figure 4.9).

The use of gel dosimetry is considered feasible for the verification of dynamic deliveries (Ceberg 2010, Ceberg *et al.* 2008, Gustavsson *et al.* 2003). It may also have an important role for audits of radiotherapy institutions participating in multicentre trials. Such trials could constitute the task of delivering a given absorbed dose to a specific volume inside an anthropomorphic phantom. To fully evaluate the entire treatment process, it is essential that all work tasks is performed by the group of staff that would be involved in the actual treatment of a patient. The treatment scenarios of the multicentre study should be mimicked to the greatest possible extent, which could be a difficult task if, for example, fiducial markers are used in the clinical setting.

Image-guided radiotherapy (IGRT) has been widely adopted to minimise the effects of inter-fractional motion. Intraprostatic gold fiducial markers are the most widespread approach for IGRT of the prostate in clinical practice (Kupelian *et al.* 2008). A pre-study was undertaken to investigate the feasibility of a normoxic polyacrylamide gel (nPAG) dosimeter with implanted gold fiducial markers for auditing purposes (**V**).

The phantom in this study consisted of three parts: the patient-simulating volume (which provided realistic scatter conditions and weight), a glass bottle containing the

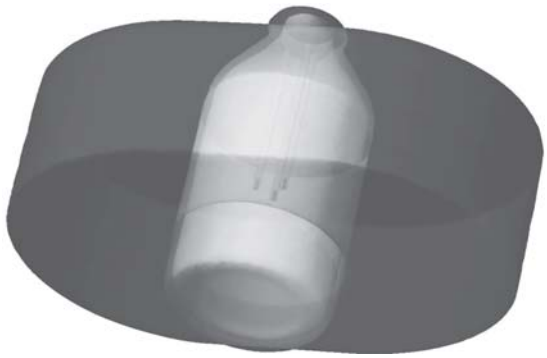

Figure 4.10. Illustration of the oval-shaped phantom, the bottle containing the normoxic polyacrylamide gel, and the fiducials attached to the fiducial support structure.

active dosimetric volume, and the fiducial markers and fiducial support structure (figure 4.10). The oval-shaped outer part of the phantom was made of polystyrene. A hole in the centre of the polystyrene fitted an oxygen-resistant glass bottle containing the nPAG gel. The fiducial markers (1 mm diameter, 5 mm length) were fixed at the ends of three PMMA rods (5 mm thickness) attached to the lid of the bottle.

A five field, 6 MV, sliding-window IMRT treatment plan was created on the phantom using internal structures (planning target volume, clinical target volume, rectum, femur heads, and urinary bladder) from a clinical case. A Clinac 2100C/D (Varian medical systems) equipped with an x-ray on-board imager was used for treatment delivery. The phantom was intentionally placed at an offset position from iso-center, with a rotation of the glass bottle around the longitudinal axis. Planar imaging at 0° and 270° using the on-board imager was undertaken, and the integrated automatic correction possibilities (longitudinal, lateral, and vertical couch movement) in the Aria verification system were used to correct for the simulated misplacement.

The gel dosimeter was read-out using a 1.5 T MRI unit (Siemens Medical Systems) and a 32-echo multi spin echo sequence. The voxel size was 1×1×3 mm, and an application software developed in-house was used to calculate R2 (Karlsson 2007). The gel results were normalised to a TPS-calculated absorbed dose using a region of homogenous dose in a slice without the presence of the fiducial markers or fiducial support structure.

Overlay of the 95% isosurface of the TPS-calculated dose distribution and the measured dose distribution using gel showed good agreement in 3D. The volume included in the 95% isosurface was approximately 3% smaller for the measured

Figure 4.11. Illustration of the anthropomorphic phantom.

distribution than the calculated distribution. An increase of the R2 value was apparent in the region surrounding the fiducial support structure. This MRI read-out artifact typically corresponded to a relative dose increase of 25% in a radius of 1 cm around the structure compared with the TPS-calculated dose distribution. However, this effect did not compromise the determination of the location of the 95% isodose surface, as the fiducial markers were located centrally in the volume of interest. Therefore, it was confirmed that MRI-based nPAG gel dosimetry can be used to verify setup correction procedures using implanted gold fiducial markers if the region in the proximity of the fiducial markers is of minor importance. For the case used in this pre-study, it was shown that the use of on-board imaging and integrated setup correction tools could be used to compensate for a deliberately introduced offset in the position of the clinical target volume.

To allow more realistic simulations of patient treatments, an anthropomorphic phantom was developed for use in audits (figure 4.11). The insert holding the gel dosimetry bottle is modular, allowing displacements and rotations of the bottle to simulate inter-fractional motion. The developed phantom will be used in future work and for audits of the centres participating in the randomised multicentre phase III study of patients with intermediate-risk prostate (HYPO-PC-RT 2008).

5 Summary and conclusions

Several tools have been developed and evaluated within the framework of this thesis. These tools have two important applications: routine use in daily clinical practice, and during the introduction of new technologies in the local clinical setting.

The concept for ensuring data integrity proposed in this thesis is based on the DICOM global information standard, and is therefore generally applicable to most radiotherapy computer systems. This developed tool can be used to analyse the compatibility between systems. After acknowledging potential systematic discrepancies, it could be used to monitor patient-specific treatment parameters. By allowing a normal condition to be defined for each system combination, the operator can be alerted only when a special cause variation arises. Otherwise, this information is likely to be rendered undetectable by rounding issues and other integrity failures that do not affect the patient safety.

The need for data transfer QA programs in the modern radiotherapy process, which includes electronically transferred information, has been recognised during the last decade. Some organisations and publications provide checklists of the steps that must be taken to ensure a high level of data integrity. However, the clinical implementation of the tests described in these recommendations requires new, efficient tools like those developed in this thesis.

Independent MU verifications can prevent major radiotherapy accidents. In this thesis it has also been demonstrated that independent MU verification data can be used to detect small changes in the treatment preparation steps if the data is monitored using SPC and control charts. Control charts also allow for statistically relevant limits to be defined for deviations between the primary TPS and the independent calculation software.

Time-resolved dosimetry was shown to be a valuable tool for real-time *in vivo* treatment monitoring. If the radiation dosimeters are integrated with interstitial localisation devices, the extra resources required for *in vivo* dosimetry will be small. Computers are today fast enough to allow evaluations of *in vivo* dosimetry data in real-time, allowing treatments to be terminated if errors are detected. This functionality may provide such confidence that patient-specific pre-treatment QA

programs can be reduced, or even replaced. Still, pre-treatment measurements on a control point level are important for detailed analyses. These analyses may result in a better understanding of the reasons why some treatment plans are associated with a low gamma pass rate. TPS vendors should provide tools for the calculation and export of dose matrices on a control point basis, allowing for these types of analyses in clinical routine and resulting in more rigorous QC and improved patient safety.

Gel dosimetry and anthropomorphic phantoms were demonstrated to be important tools for complete end-to-end tests. Such tools are especially important when introducing new technologies. The technique allows for full 3D comparisons of the planned and delivered dose distributions. The MR artifacts introduced by fiducial markers have little impact on the analysis if the proximity of the fiducial markers is of minor dosimetric importance.

The methods and concepts developed in this thesis for the QC of the physical aspects of patient-specific treatment parameters can improve patient safety and reduce the resources required for a comprehensive QA program.

6 Acknowledgements

First of all, I would like to thank my supervisors Sven ÅJ Bäck and Crister Ceberg. Sven, you are always enthusiastic and have encouraged me to undertake my own initiatives. Crister, you always take time for discussions and your ideas have been much appreciated.

I would like to acknowledge the following sources of financial support: The Swedish Cancer Society, The Cancer Foundation at Skåne University Hospital in Malmö, and The Cancer Research Foundation at the Department of Oncology (Malmö University Hospital).

A special thanks to Sacha af Wetterstedt, who greatly contributed to two of the papers, for many interesting discussions. I look forward to a continuation of our collaboration. Thanks also to Sofie Ceberg for introducing me to gel dosimetry, and for our exciting adventures at conferences in Europe and the United States.

I am very grateful to the co-authors, institutions, and colleagues that have contributed to this work. Many thanks to the treatment planners (Malin, Pia, Marie, and Marlene) for assistance during the projects; to Sven Brink for the development of phantoms and all daily support; and to all my colleagues, former colleagues, and friends at the Department of Radiation Physics (Skåne University Hospital) who have supported this work and shared their knowledge (Helen, Anna, Elias, Lotta, Hilko, Stefan, *et al.*).

I also express my gratitude to the head of the department during most of my Ph.D., Professor Sören Mattsson. You always have the greatest faith in people, and have created a friendly and open research environment.

Thanks to all of my colleagues and friends at the Department of Medical Radiation Physics (Lund University): Christopher, Andreas, Christian, Carl, Pontus, Tony, Marcus, Marie, Daniel, Maria, Pernilla, Therése, Magnus, Mattias, Mats, Hanna, Ünal, Martin, *et al.*

Last, but not least, I would like to thank my family and friends for their support.

7 References

AAPM (2005). *American Association of Physicists in Medicine Report no. 87: Diode in vivo dosimetry for patients receiving external beam radiation therapy*, Madison: Medical Physics Publishing.

Abdel-Wahab, M., Rengan, R., Curran, B., Swerdloff, S., Miettinen, M., Field, C., Ranjitkar, S., Palta, J. and Tripuraneni, P. (2010). Integrating the healthcare enterprise in radiation oncology plug and play–the future of radiation oncology?, *Int J Radiat Oncol Biol Phys* **76**(2): 333–336.

Ash, D. and Bates, T. (1994). Report on the clinical effects of inadvertent radiation underdosage in 1045 patients, *Clin Oncol* **6**(4): 214–226.

Baldock, C., Deene, Y. D., Doran, S., Ibbott, G., Jirasek, A., Lepage, M., McAuley, K. B., Oldham, M. and Schreiner, L. J. (2010). Polymer gel dosimetry, *Phys Med Biol* **55**(5): R1–63.

Bedford, J. L., Lee, Y. K., Wai, P., South, C. P. and Warrington, A. P. (2009). Evaluation of the Delta4 phantom for IMRT and VMAT verification, *Phys Med Biol* **54**(9): N167–N176.

Brahme, A. (1984). Dosimetric precision requirements in radiation therapy, *Acta Radiol Oncol* **23**(5): 379–391.

Buonamici, F. B., Compagnucci, A., Marrazzo, L., Russo, S. and Bucciolini, M. (2007). An intercomparison between film dosimetry and diode matrix for IMRT quality assurance, *Med Phys* **34**(4): 1372–1379.

Calandrino, R., Cattaneo, G. M., Fiorino, C., Longobardi, B., Mangili, P. and Signorotto, P. (1997). Detection of systematic errors in external radiotherapy before treatment delivery, *Radiother Oncol* **45**(3): 271–274.

Carver, A., Gilmore, M., Riley, S., Uzan, J. and Mayles, P. (2011). An analytical approach to acceptance criteria for quality assurance of intensity modulated radiotherapy, *Radiother Oncol* **100**(3): 453–455.

Ceberg, S. (2010). *3D verification of dynamic and breathing adapted radiotherapy using polymer gel dosimetry*, PhD thesis, Lund University. http://umu.diva-portal.org/

Ceberg, S., Karlsson, A., Gustavsson, H., Wittgren, L. and Bäck, S. Å. J. (2008). Verification of dynamic radiotherapy: the potential for 3D dosimetry under respiratory-like motion using polymer gel, *Phys Med Biol* **53**(20): N387–N396.

Cherpak, A., Ding, W., Hallil, A. and Cygler, J. E. (2009). Evaluation of a novel 4D in vivo dosimetry system, *Med Phys* **36**(5): 1672–1679.

Clark, B. G., Brown, R. J., Ploquin, J. L., Kind, A. L. and Grimard, L. (2010). The management of radiation treatment error through incident learning, *Radiother Oncol* **95**(3): 344–349.

Cunningham, J., Coffey, M., Knöös, T. and Holmberg, O. (2010). Radiation Oncology Safety Information System (ROSIS)–profiles of participants and the first 1074 incident reports, *Radiother Oncol* **97**(3): 601–607.

Damkjær, S. M. S. (2011). *Time-Resolved Luminescence Dosimetry using Fiber-Coupled Al_2O_3:C and Applications in External Beam Radiotherapy*, PhD thesis, University of Copenhagen. http://www.nbi.ku.dk/english/research/phd_theses/phd_theses_2011/sidsel_damkjaer/Sidsel_Damkjaer.pdf

de la Vega, J. M., Martínez-Luna, R. J., Guirado, D., Vilches, M. and Lallena, A. M. (2012). Statistical control of the spectral quality index in electron beams, *Radiother Oncol* **102**(3): 406–411.

Delaney, G., Jacob, S., Featherstone, C. and Barton, M. (2005). The role of radiotherapy in cancer treatment: estimating optimal utilization from a review of evidence-based clinical guidelines, *Cancer* **104**(6): 1129–1137.

Derreumaux, S., Etard, C., Huet, C., Trompier, F., Clairand, I., Bottollier-Depois, J.-F., Aubert, B. and Gourmelon, P. (2008). Lessons from recent accidents in radiation therapy in France, *Radiat Prot Dosimetry* **131**(1): 130–135.

DOH (2007). *On the state of public health: Annual report of the Chief Medical Officer 2006, Chapter 5: Radiotherapy: Hidden Dangers*, London: Department of Health. http://www.dh.gov.uk/prod_consum_dh/groups/dh_digitalassets/@dh/@en/documents/digitalasset/dh_076852.pdf

Dutreix, A., Bjärngard, B. E., Bridier, A., Mijhheer, B., Shaw, J. E. and Svensson, H. (1997). *Monitor unit calculation for high energy photon, Physics for clinical radiotherapy - ESTRO Booklet Report No. 3*, Brussels: European Society for Therapeutic Radiology and Oncology.

Essers, M. and Mijnheer, B. J. (1999). In vivo dosimetry during external photon beam radiotherapy, *Int J Radiat Oncol Biol Phys* **43**(2): 245–259.

Feygelman, V., Zhang, G., Stevens, C. and Nelms, B. E. (2011). Evaluation of a new VMAT QA device, or the "X" and "O" array geometries, *J Appl Clin Med Phys* **12**(2): 146–168.

Fiorino, C., Corletto, D., Mangili, P., Broggi, S., Bonini, A., Cattaneo, G. M., Parisi, R., Rosso, A., Signorotto, P., Villa, E. and Calandrino, R. (2000). Quality assurance by systematic in vivo dosimetry: results on a large cohort of patients, *Radiother Oncol* **56**(1): 85–95.

Fong, P. M., Keil, D. C., Does, M. D. and Gore, J. C. (2001). Polymer gels for magnetic resonance imaging of radiation dose distributions at normal room atmosphere, *Phys Med Biol* **46**(12): 3105–3113.

General Inspectorate of Social Affairs (2007). *Summary of ASN report n° 2006 ENSTR 019 - IGAS n° RM 2007-015P on the Epinal radiotherapy accident*. http://www.asn.fr/index.php/content/download/15545/100850/ASN_report_n_2006_ENSTR_019_-_IGAS.pdf

Goitein, M. (1983). Nonstandard deviations, *Med Phys* **10**(5): 709–711.

Gustavsson, H., Karlsson, A., Bäck, S. Å. J., Olsson, L. E., Haraldsson, P., Engström, P. and Nyström, H. (2003). MAGIC-type polymer gel for three-dimensional dosimetry: intensity-modulated radiation therapy verification, *Med Phys* **30**(6): 1264–1271.

Holmberg, O. (2007). Accident prevention in radiotherapy, *Biomed Imaging Interv J* **3**(2): e27.

Holmberg, O. and McClean, B. (2002). Preventing treatment errors in radiotherapy by identifying and evaluating near misses and actual incidents, *Journal of Radiotherapy in Practice* **3**: 13–26.

Huang, G., Medlam, G., Lee, J., Billingsley, S., Bissonnette, J.-P., Ringash, J., Kane, G. and Hodgson, D. C. (2005). Error in the delivery of radiation therapy: results of a quality assurance review, *Int J Radiat Oncol Biol Phys* **61**(5): 1590–1595.

HYPO-PC-RT (2008). *Phase III study of HYPOfractionated RadioTherapy of intermediate risk localised Prostate Cancer*. http://www.controlled-trials.com/ISRCTN45905321

IAEA (2000a). *Technical Reports Series No. 398: Absorbed Dose Determination in External Beam Radiotherapy - An International Code of Practice for Dosimetry Based on Standards of Absorbed Dose to Water*, Vienna: International Atomic Energy Agency.

IAEA (2000b). *Safety Reports Series No. 17: Lessons learned from accidental exposures in radiotherapy*, Vienna: International Atomic Energy Agency. http://www-pub.iaea.org/MTCD/Publications/PDF/Pub1084_web.pdf

IAEA (2005). *Radiation Oncology Physics: A Handbook for Teachers and Students*, Vienna: International Atomic Energy Agency. http://www-pub.iaea.org/mtcd/publications/pdf/pub1196_web.pdf

IAEA (training material). *Prevention of Accidental Exposure in Radiotherapy*. https://rpop.iaea.org/RPOP/RPoP/Content/AdditionalResources/Training/1_TrainingMaterial/AccidentPreventionRadiotherapy.htm

ICAO (2011). *2011 State of Global Aviation Safety*, Montréal: International Civil Aviation Organization. http://www.icao.int/safety/Documents/ICAO_State-of-Global-Safety_web_EN.pdf

Isbakan, F., Ulgen, Y., Bilge, H., Ozen, Z., Agus, O. and Buyuksarac, B. (2007). Gamma Knife 3-D dose distribution near the area of tissue inhomogeneities by normoxic gel dosimetry, *Med Phys* **34**(5): 1623–1630.

Karlsson, A. (2007). *Characterization and clinical application of normoxic polymer gel in radiation therapy dosimetry*, PhD thesis, Lund University.

Keall, P. and Baldock, C. (1999). A theoretical study of the radiological properties and water equivalence of Fricke and polymer gels used for radiation dosimetry, *Australas Phys Eng Sci Med* **22**(3): 85–91.

Kindblom, J., Ekelund-Olvenmark, A-M., Syren, H., Iustin, R., Braide, K., Frank-Lissbrant, I. and Lennernäs, B. (2009). High precision transponder localization using a novel electromagnetic positioning system in patients with localized prostate cancer, *Radiother Oncol* **90**(3): 307–311.

Knöös, T., Johnsson, S. A., Ceberg, C. P., Tomaszewicz, A. and Nilsson, P. (2001). Independent checking of the delivered dose for high-energy X-rays using a hand-held PC, *Radiother Oncol* **58**(2): 201–208.

Korreman, S., Medin, J. and Kjaer-Kristoffersen, F. (2009). Dosimetric verification of RapidArc treatment delivery, *Acta Oncol* **48**(2): 185–191.

Kung, J. H., Chen, G. T. Y. and Kuchnir, F. K. (2000). A monitor unit verification calculation in intensity modulated radiotherapy as a dosimetry quality assurance, *Med Phys* **27**(10): 2226–2230.

Kupelian, P. A., Langen, K. M., Willoughby, T. R., Zeidan, O. A. and Meeks, S. L. (2008). Image-guided radiotherapy for localized prostate cancer: treating a moving target, *Semin Radiat Oncol* **18**(1): 58–66.

Lanson, J. H., Essers, M., Meijer, G. J., Minken, A. W., Uiterwaal, G. J. and Mijnheer, B. J. (1999). In vivo dosimetry during conformal radiotherapy: requirements for and findings of a routine procedure, *Radiother Oncol* **52**(1): 51–59.

Law, M. Y. Y. and Liu, B. (2009). Informatics in radiology: DICOM-RT and its utilization in radiation therapy, *Radiographics* **29**(3): 655–667.

Leunens, G., Verstraete, J., den Bogaert, W. V., Dam, J. V., Dutreix, A. and van der Schueren, E. (1992). Human errors in data transfer during the preparation and delivery of radiation treatment affecting the final result: "garbage in, garbage out", *Radiother Oncol* **23**(4): 217–222.

Low, D. A., Harms, W. B., Mutic, S. and Purdy, J. A. (1998). A technique for the quantitative evaluation of dose distributions, *Med Phys* **25**(5): 656–661.

MacKay, R. I. and Williams, P. C. (2009). The cost effectiveness of in vivo dosimetry is not proven, *Br J Radiol* **82**(976): 265–266.

McDermott, L. N., Wendling, M., Sonke, J-J., van Herk, M. and Mijnheer, B. J. (2007). Replacing pretreatment verification with in vivo EPID dosimetry for prostate IMRT, *Int J Radiat Oncol Biol Phys* **67**(5): 1568–1577.

McKenzie, A., Briggs, G., Buchanan, R., Harvey, L., Iles, A., Kirby, M., Mayles, P., Thomas, S. and Williams, M. (2006). *Balancing Costs and Benefits of Checking in Radiotherapy*, York.

Mijnheer, B. J., Battermann, J. J. and Wambersie, A. (1987). What degree of accuracy is required and can be achieved in photon and neutron therapy?, *Radiother Oncol* **8**(3): 237–252.

Montgomery, D. C. (1996). *Introduction to statistical quality control*, Hoboken: John Wiley & Sons.

Munro, A. J. (2007). Hidden danger, obvious opportunity: error and risk in the management of cancer, *Br J Radiol* **80**(960): 955–966.

NEMA (2011). *Digital Imaging and Communications in Medicine (DICOM)*, Rosslyn: National Electrical Manufacturers Association. ftp://medical.nema.org/medical/dicom/2011

New York State Department of Health (2005). *LINAC/IMRT Significant Misadministration - Software Error Suspected (Notice No. BERP 2005-1)*, New York:

New York State Department of Health. http://www.health.ny.gov/environmental/radiological/radon/radioactive_material_licensing/docs/berp2005_1.pdf

Noel, A., Aletti, P., Bey, P. and Malissard, L. (1995). Detection of errors in individual patients in radiotherapy by systematic in vivo dosimetry, *Radiother Oncol* **34**(2): 144–151.

Nyholm, T. (2008). *Verification of dose calculations in radiotherapy*, PhD thesis, Umeå University. http://urn.kb.se/resolve?urn=urn:nbn:se:umu:diva-1931

Nyholm, T., Olofsson, J., Ahnesjö, A. and Karlsson, M. (2006). Photon pencil kernel parameterisation based on beam quality index, *Radiother Oncol* **78**(3): 347–351.

Patton, G. A., Gaffney, D. K. and Moeller, J. H. (2003). Facilitation of radiotherapeutic error by computerized record and verify systems, *Int J Radiat Oncol Biol Phys* **56**(1): 50–57.

Pawlicki, T. and Whitaker, M. (2008). Variation and control of process behavior, *Int J Radiat Oncol Biol Phys* **71**(1 Suppl): S210–S214.

Pawlicki, T., Whitaker, M. and Boyer, A. L. (2005). Statistical process control for radiotherapy quality assurance, *Med Phys* **32**(9): 2777–2786.

Pawlicki, T., Yoo, S., Court, L. E., McMillan, S. K., Rice, R. K., Russell, J. D., Pacyniak, J. M., Woo, M. K., Basran, P. S., Boyer, A. L. and Bonilla, C. (2008b). Process control analysis of IMRT QA: implications for clinical trials, *Phys Med Biol* **53**(18): 5193–5205.

Pawlicki, T., Yoo, S., Court, L. E., McMillan, S. K., Rice, R. K., Russell, J. D., Pacyniak, J. M., Woo, M. K., Basran, P. S., Shoales, J. and Boyer, A. L. (2008). Moving from IMRT QA measurements toward independent computer calculations using control charts, *Radiother Oncol* **89**(3): 330–337.

Petoukhova, A. L., van Egmond, J., Eenink, M. G. C., Wiggenraad, R. G. J. and van Santvoort, J. P. C. (2011). The ArcCHECK diode array for dosimetric verification of HybridArc, *Phys Med Biol* **56**(16): 5411–5428.

Pisaturo, O., Moeckli, R., Mirimanoff, R-O. and Bochud, F. O. (2009). A Monte Carlo-based procedure for independent monitor unit calculation in IMRT treatment plans, *Phys Med Biol* **54**(13): 4299–4310.

RCR (2008). *The Royal College of Radiologists, Society and College of Radiographers, Institute of Physics and Engineering in Medicine, National Patient Safety Agency, Brittish Institute of Radiology. Towards Safer Radiotherapy*, London: The Royal College of Radiologists. https://www.rcr.ac.uk/docs/oncology/pdf/Towards_saferRT_final.pdf

Saw, C., Ferenci, M. and Wanger, H. (2008). Technical aspects of quality assurance in radiation oncology, *Biomed Imaging Interv J* **4**(3): e48.

SBU (2003). *Radiotherapy for Cancer: A Systematic Literature Review*, Stockholm: The Swedish Council on Technology Assessment in Health Care. http://www.sbu.se/en/Published/Yellow/Radiotherapy-for-cancer/

Scottish ministers for the ionising radiation (medical exposures) regulations (2006). *Unintended overexposure of patient Lisa Norris during radiotherapy treatment at the Beatson Oncology Centre, Glasgow in January 2006*. http://www.scotland.gov.uk/Publications/2006/10/27084909/0

Sellakumar, P., Arun, C., Sanjay, S. S. and Ramesh, S. B. (2011). Comparison of monitor units calculated by radiotherapy treatment planning system and an independent monitor unit verification software, *Phys Med* **27**(1): 21–29.

Shafiq, J., Barton, M., Noble, D., Lemer, C. and Donaldson, L. J. (2009). An international review of patient safety measures in radiotherapy practice, *Radiother Oncol* **92**(1): 15–21.

Shah, A. P., Kupelian, P. A., Willoughby, T. R., Langen, K. M. and Meeks, S. L. (2011). An evaluation of intrafraction motion of the prostate in the prone and supine positions using electromagnetic tracking, *Radiother Oncol* **99**(1): 37–43.

Shewhart, W. (1931). *Economic control of quality of manufactured product*, Princeton: D. Van Nostrand Company, Inc.

Siochi, R. A., Balter, P., Bloch, C. D., Santanam, L., Blodgett, K., Curran, B. H., Engelsman, M., Feng, W., Mechalakos, J., Pavord, D., Simon, T., Sutlieff, S. and Zhu, X. R. (2011). A rapid communication from the AAPM Task Group 201: recommendations for the QA of external beam radiotherapy data transfer. AAPM TG 201: quality assurance of external beam radiotherapy data transfer, *J Appl Clin Med Phys* **12**(1): 170–181.

Stapenhurst, T. (2005). *Mastering statistical process control*, Oxford: Elsevier Butterworth-Heinemann.

Stern, R. L., Heaton, R., Fraser, M. W., Goddu, S. M., Kirby, T. H., Lam, K. L., Molineu, A., Zhu, T. C. and AAPM Task Group 114 (2011). Verification of monitor unit calculations for non-IMRT clinical radiotherapy: report of AAPM Task Group 114, *Med Phys* **38**(1): 504–530.

Swerdloff, S. J. (2007). Data handling in radiation therapy in the age of image-guided radiation therapy, *Semin Radiat Oncol* **17**(4): 287–292.

Vergote, K., Deene, Y. D., Duthoy, W., Gersem, W. D., Neve, W. D., Achten, E. and Wagter, C. D. (2004). Validation and application of polymer gel dosimetry for the dose verification of an intensity-modulated arc therapy (IMAT) treatment, *Phys Med Biol* **49**(2): 287–305.

VMS (2011). *100013698-05 DynaLog File Viewer Reference Guide*, Palo Alto: Varian Medical Systems.

WHO (2008). *Radiotherapy Risk Profile - Technical Manual*, Geneva: World Health Organization. http://www.who.int/patientsafety/activities/technical/radiotherapy_risk_profile.pdf

Williams, M. V. and McKenzie, A. (2008). Can we afford not to implement in vivo dosimetry?, *Br J Radiol* **81**(969): 681–684.

Paper I

Radiotherapy and Oncology xxx (2012) xxx–xxx

Contents lists available at SciVerse ScienceDirect

Radiotherapy and Oncology

journal homepage: www.thegreenjournal.com

Original article

Ensuring the integrity of treatment parameters throughout the radiotherapy process

Fredrik Nordström [a,*], Crister Ceberg [b], Sven Å.J. Bäck [a,c]

[a] Department of Medical Radiation Physics, Lund University, Malmö; [b] Department of Medical Radiation Physics, Lund University, Lund; [c] Department of Radiation Physics, Skåne University Hospital, Malmö, Sweden

ARTICLE INFO

Article history:
Received 1 August 2011
Received in revised form 2 January 2012
Accepted 2 January 2012
Available online xxxx

Keywords:
Data integrity
Data transfer
Risk management
Patient safety
DICOM-RT

ABSTRACT

Background and purpose: Ensuring data integrity in radiotherapy is of major importance and a complex task. The aim of this study was to compare three different combinations of treatment planning and record and verify systems with respect to data integrity.

Materials and methods: A software for comparison of treatment parameters in DICOM-RT files was developed using the MATLAB R2010a (MathWorks Inc.) environment. One hundred treatment plans were analyzed for each system combination. In the first step of the analysis, all parameters were compared and a normal condition for each system combination was identified. The second step focused on the discovery of potential special cause deviations, e.g. by applying tolerance levels.

Results: In total, 15% and 0.37% of all comparisons failed to meet the defined integrity demands in step 1 and step 2 of the analysis, respectively. Differences in the data integrity level between the systems were observed, ranging on average from 3.1 to 11.9 discrepancies per beam for the different RV-TPS combinations.

Conclusions: The proposed method can be used to increase the safety for individual patients by ensuring that the intended treatment is delivered. The system combination with the highest level of data integrity was found to be the one which shares a single database.

Preparation and planning for radiotherapy is a complex procedure. At some point in the process, data often have to be transfered between software and computer systems from different vendors. To allow different medical systems to communicate with each other, a global information-technology standard, Digital Imaging and Communications in Medicine (DICOM) has been developed [1]. In 1993 DICOM v3.0 was released, which encompasses both communication protocols and file formats, allowing DICOM to act as a base for intersystem transfer of digital medical images. The standard was extended in 1997 to cover radiotherapy information objects [2]. This extension is referred to as DICOM-RT. Today DICOM-RT has been widely accepted and has a major role in the communication between different radiotherapy systems. An initiative to help users and vendors to develop approaches for integrating various radiation oncology systems (IHE-RO) has also been launched where DICOM is an integral part [3]. Undoubtedly, the absence of manual data transfer ensures a higher level of data integrity [4]. However, manual data input might be difficult to avoid at some steps of the treatment chain, which inevitably leads to an increased risk [5,6]. There is also a possibility that data might be lost or misinterpreted because different systems might not fully support the same data structures of the DICOM standard [7].

Some systems are developed to suit one specific isolated task, but more often systems are able to perform different tasks and the functionality of different systems in the RT environment tends to overlap. For instance, in many clinical environments, beams can be created and shaped in both the treatment planning system (TPS) and in the record and verify (RV) system. The user is able to edit data as well as add complementary information in several systems. For the individual user the relevance and consistency of these data changes are not always clear, which may result in unwanted consequences [8]. The transfer of treatment parameters between different systems during the radiotherapy process could potentially introduce discrepancies between datasets [9]. In fact, the World Health Organization (WHO) has reported that the greatest bulk of incidents in modern radiotherapy without any known adverse events to patients are related to the transfer of information (38%) [9,10]. Thus, there is an obvious need to ensure, in every situation, that the intended (signed/approved) treatment plan also is delivered to the patient.

Modern computer systems often rely on checksums, which are fixed-sized signatures calculated from a block of digital data. One of the most commonly used algorithms for calculation of check sum is the cyclic redundancy check (CRC) [11]. By comparing check sums before and after transmission or storage, communication errors may be detected. However, this method is not applicable for comparison of the data in systems from different vendors, as

* Corresponding author.
E-mail address: Fredrik.Nordstrom@med.lu.se (F. Nordström).

0167-8140/$ - see front matter © 2012 Elsevier Ireland Ltd. All rights reserved.
doi:10.1016/j.radonc.2012.01.004

Please cite this article in press as: Nordström F et al. Ensuring the integrity of treatment parameters throughout the radiotherapy process. Radiother Oncol (2012), doi:10.1016/j.radonc.2012.01.004

the checksum needs to be calculated from exactly the same data to pass the test. If data are modified or added, the test will always fail, without providing any information on what part of the data has been altered. In order to manage data integrity issues in radiotherapy, new tools are needed [12]. Such tools could be implemented into a software application to monitor alterations of the patient specific treatment data and thereby improve the patient safety. The recent rapid communication from the AAPM Task Group (TG) 201 provides clinics with a checklist that could be used in the design of data transfer related QA processes [13]. A method for comparisons of ASCII files following the RTPConnect Radiotherapy Treatment Planning Import/Export Interface Specification (IMPAC) and Pinnacle3 (Philips Healthcare) data files has been shown to be an efficient method for automatic one-to-one data correspondence checks [14].

The aim of this study was to compare different combinations of TPS and RV systems with respect to data integrity in a clinical multi-vendor environment. A general method based on the DICOM standard was developed to compare treatment data from different steps of the treatment chain in order to verify the integrity of datasets. Clinical implementations of this method could constitute an integral part of a QA program based on the TG 201 recommendations.

Materials and methods

By comparing exported DICOM files, the data in the systems are indirectly compared and the integrity of the data between systems is thus verified (Fig. 1). A requisite for this method is that the exported DICOM data from the systems corresponds to the data in the databases of the systems. The vendors should check that the exported information complies with the communication protocol standards (e.g. DICOM) by testing of the output information [15,16]. However, users are advised to test the DICOM compatibility as a part of the commissioning of the systems [13].

Comparison of DICOM attributes

A software for comparison of treatment parameters in DICOM-RT files was developed using the MATLAB R2010a (MathWorks Inc.) environment. The *dicominfo* function and the default DICOM data dictionary in the Image Processing Toolbox were used for extraction of metadata from the DICOM-files. Each attribute in the DICOM file is identified by a 2-byte integer group number and a 2-byte integer element number which together are referred to as a tag [17].

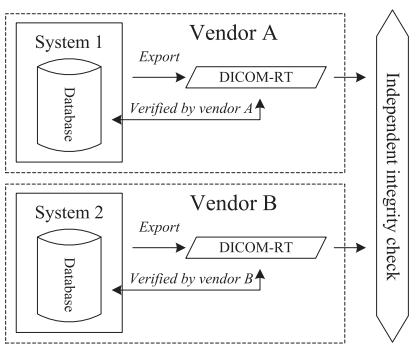

Fig. 1. An illustration of the concept of data integrity verification using the proposed model.

The DICOM attributes directly related to the treatment unit setting and identification of treatment devices (e.g. blocks, boli) were identified from the DICOM standard [1]. The *Patient ID* and *RT Plan Label* were used to pair corresponding treatment plans from different systems. The *Beam Number* was used to pair corresponding beam data. If system designs or clinical procedures do not allow a robust beam numbering that does not change between systems, an alternative method for beam matching could be used [14]. All DICOM attributes considered in the plan comparison can be found in Supplementary material, which also illustrates the hierarchy of the data. Only external photon beam therapy was considered in this study.

The *Beam Sequence* in the DICOM-RT Plan defines equipment parameters for delivery of external radiation beams. Each *Beam Sequence* item contains a *Control Point Sequence*, which is a sequence of machine configurations describing the treatment beam. All applicable parameters are specified at the first control point, with the exception of couch positions which are omitted in the first control point if relative coordinates are used. The parameters that change at any control point should be specified explicitly at all control points. Only treatment beams (i.e. beams where *Treatment Delivery Type* is not defined or the value is TREATMENT) are compared. The *Number of Beams* attribute is modified accordingly to reflect the number of treatment beams in comparison.

Owing to some flexibility in the standard, all DICOM attributes cannot be compared on an entry-by-entry basis. To verify the integrity of monitor units (MUs), the total MUs for each beam as defined in the *Fraction Group Sequence*, as well as the number of delivered monitor units at each control point are compared. The number of MUs delivered at each control point is calculated according to Eq. (1), where i denotes the beam and j the control point [1]:

$$\mathrm{MU}_{i,j} = \mathit{Beam\ Meterset}_i \cdot \frac{\mathit{Cumulative\ Meterset\ Weight}_{i,j}}{\mathit{Final\ Cumulative\ Meterset\ Weight}_i} \qquad (1)$$

The beam number is used as a link between the fractionation data in the *Fraction Group Sequence* and a specific item in the *Beam Sequence*. Similar relationships exist for wedge data, which are defined under the *Wedge Sequence* and the position of the wedge is then defined in the *Wedge Position Sequence* under the *Control Point Sequence*. The *Wedge Number* links this information together. In the developed software, the linking of information is performed before it is compared between systems. For wedged beams the control point items might need to be rearranged in the comparison and the control points that do not contribute to the treatment be deleted (i.e. zero MU delivery). In such cases the affected parameters (i.e. *Number of Control Points* and *Control Point Index*) are modified accordingly.

The position of the collimators is defined in the *Beam Limiting Device Position Sequence*. An item in this sequence corresponds either to the X-jaws, Y-jaws or the multi-leaf collimator (MLC). The software compares all defined collimator positions.

Add-on accessories such as compensators, blocks, trays, external wedges and boli constitute treatment equipment that is identified by codes or user notes and plans utilizing these items might be subjected to compromised integrity at a higher level during inter-system transfer. The software verifies that the identification data and the position of each accessory are the same for the two plans. The physical properties of the block and compensator usually only needs to be transfered to software involved in the manufacturing process of the accessory under consideration. In general, these software do not support DICOM export and it is therefore not possible

Please cite this article in press as: Nordström F et al. Ensuring the integrity of treatment parameters throughout the radiotherapy process. Radiother Oncol (2012), doi:10.1016/j.radonc.2012.01.004

to use the proposed method to verify the data integrity of this information.

Patient setup parameters are not compared using the proposed method, since these are usually dependent on notes and the structure of patient setup information is not strictly defined. *The RT Patient Setup Module* allows detailed description of the patient setup. However, the complexity level of this information is much higher compared to the *RT Beam Module* attributes, which makes a compromised integrity more likely.

All other *Beam Sequence* and *Control Point Sequence* item attributes are verified entry-by-entry. In total, comparisons of 61 parameters based on the DICOM-attributes were implemented in the software.

By using a tolerance level in the comparison of each numerical data value, rounding issues without any significance for the treatment outcome could be taken into account.

Comparisons of different TPS-RV combinations

The developed software was implemented in a clinical environment. A migration from the RV-system Visir (Nucletron) to Aria (Varian Medical Systems), as well as a migration from the TPS MasterPlan (Nucletron) to Eclipse (Varian) allowed an intercomparison study between three different system combinations (MasterPlan → Visir, MasterPlan → Aria and Eclipse → Aria) within the same clinical environment.

One hundred treatment plans, including both 3D-conformal radiotherapy (3D-CRT) and intensity modulated radiotherapy (IMRT) plans, were analyzed for each system combination. The approved plan generated using the TPS (MasterPlan or Eclipse) was compared with the treated plan as registered in the RV system (Visir or Aria) after treatment completion. Both plans were exported to the comparison software as DICOM-RT Plan objects. Each system combination had been in clinical routine for at least one year when, after an otherwise random time point, the next 100 consecutive approved plans were included in the study.

The average number of beams per plan for different system combinations ranged between 3.9 and 4.6. 40 beams had a shape that was only defined by the collimator jaws and 25 beams for each combination were intensity modulated. Blocks were utilized in 1 and 6 beams for the combinations MasterPlan → Visir and MasterPlan → Aria, respectively. The plans were mainly created in the TPS and additional information (e.g. dose rate for the MasterPlan combinations and block identification data) were manually added in the RV. Treatment top position data were acquired during the first treatment. In some cases, the plans were created using Advantage SIM (GE Healthcare) and exported, via DICOM, to the TPS for MU calculations. Owing to the differences in system design some variations in the clinical practice between the systems were present. The transfer of fundamental treatment parameters (e.g. treatment unit, energy, gantry angle, field size, MU) was manually checked by a medical physicist, by comparing the data in the RV with TPS printouts prior to the treatment. The light field on the treatment unit was verified against printouts of the beam outline generated in the TPS. Additional non data transfer related QA was also performed, such as an independent monitor unit calculation.

The Eclipse and Aria systems are sharing a single database. The export is therefore performed at two different points in time (after completed treatment planning and after treatment completion) from the same underlying database.

The data integrity analysis were performed in two steps. In the first step, all parameters were compared without any tolerance level and a normal condition for each system combination was identified. The normal condition constitutes clinically accepted systematic data alterations arising from software designs and/or clinical procedures. The number of deviations in this step of the analysis was used as a measure of the level of integrity for the system combination. Most comparisons are performed on a control point level and secondly on a beam level. Due to the different number of control points and beams compared for each system combination, the number of deviations needs to be normalized to either the total number of control points or the total number of beams.

In the second step, parameters were excluded if their associated DICOM attributes were missing from one or both systems. In order to isolate potential special cause deviations outside the normal conditions, tolerances were used to manage rounding of decimal values and look-up-tables were used for data that are mapped in the import and/or export in the systems. Only MLC positions for leaves defining the beam aperture shape were compared for the MasterPlan → Visir combination, as Visir does not export MLC positions outside the beam opening (i.e. MLC positions set to zero). The deviations isolated in the second step of the analysis were expected to be caused by user interventions not following clinical routines, not optimally designed clinical routines, or non-systematic data transfer issues. The potential special cause deviations discovered were classified into seven different categories depending on how they arose: treatment unit breakdowns, manual editing of data during normal circumstances, acquisition of treatment parameters, information lost during data transfer, correction of errors in treatment plan, non-linear chain of data transfer.

Root cause and consequence analysis were undertaken for all the discovered deviations.

Results

Out of the initial 61 parameters, 45 were compared at least once. The remaining parameters (listed below) were not compared due to missing corresponding DICOM attributes in all the exported DICOM files.

Wedge Accessory Code, Compensator Sequence, Compensator Description, Compensator Number, Compensator ID, Compensator Type, Compensator Accessory Code, Compensator Mounting Position, Bolus ID, Bolus Description, Bolus Accessory Code, Block Mounting Position, Table Top Pitch Angle, Table Top Pitch Rotation Direction, Table Top Roll Angle, Table Top Roll Rotation Direction.

Table top data were not available from the TPS, but acquired at the first treatment session and these parameters were therefore excluded in the second step of the analysis. This was also the case for the *Dose Rate* attribute for two of the system combinations (MasterPlan → Visir/Aria). Look-up-tables were employed in step two for the parameters *Treatment Machine Name* and *Wedge ID* after verifying that this information was correctly mapped between the systems. The decimal precision in Visir was found to be on a single MU/mm/° level and, therefore, discrepancies up to half a unit were expected. A tolerance level of half a unit was therefore used for all numerical parameters, except for the *Beam Meterset* and the *Control Point Meterset* where a 1 MU tolerance was used for all systems.

In total, 15% and 0.37% of all comparisons failed to meet the defined integrity demands in step 1 and step 2 of the analysis, respectively (Table 1).

Deviations were found for IMRT plans in the table top parameters and *Number of Fractions Planned* for all system combinations. The MasterPlan combinations also resulted in deviations in *Control Point Meterset* and *Dose Rate Set*. Deviations in jaw- and MLC-positions and *Patient Support Angle* were only observed for the combination MasterPlan → Visir.

Due to the small number of discrepancies found on a control point level, the number of discovered discrepancies in the first part of the analysis normalized to the number of beams investigated was used as a measure of the integrity level between data in the

Please cite this article in press as: Nordström F et al. Ensuring the integrity of treatment parameters throughout the radiotherapy process. Radiother Oncol (2012), doi:10.1016/j.radonc.2012.01.004

Table 1
The number of observed deviations in step 2 (step 1 within brackets) from the total number of comparisons in step 1. Deviations in step 2 are highlighted in bold.

Parameter	MasterPlan → Visir	MasterPlan → Aria	Eclipse → Aria
Treatment Machine Name	0/394 (394)	0/422 (0)	0/464 (0)
Primary Dosimeter Unit	0/394 (0)	0/422 (0)	0/464 (0)
Beam Number	0/394 (0)	0/422 (0)	0/464 (0)
Beam Name	**76/394 (76)**	0/422 (0)	0/464 (0)
Beam Type	0/394 (0)	0/422 (0)	0/464 (0)
Radiation Type	0/394 (0)	0/422 (0)	0/464 (0)
Number of wedges	0/394 (0)	0/422 (0)	0/464 (0)
Wedge Sequence	0/157 (0)	0/172 (0)	0/89 (0)
Wedge Number	0/157 (0)	0/172 (0)	0/89 (0)
Wedge Type	0/157 (0)	0/172 (0)	0/89 (0)
Wedge ID	0/157 (157)	0/172 (172)	0/89 (0)
Wedge Angle	0/157 (0)	0/172 (0)	0/89 (0)
Wedge Orientation	0/157 (0)	0/172 (0)	0/89 (0)
Number of compensators	0/394 (0)	0/422 (0)	0/464 (0)
Number of boli	0/394 (0)	**11/422 (11)**	0/464 (0)
Referenced Bolus Sequence	0/0 (0)	**11/11 (11)**	0/7 (0)
Number of blocks	0/394 (0)	0/422 (0)	0/464 (0)
Block Sequence	0/1 (0)	0/6 (0)	0/0 (0)
Block tray ID	0/1 (1)[a]	0/6 (6)[a]	0/0 (0)
Block Accessory Code	0/0 (0)	0/6 (6)[a]	0/0 (0)
Block Number	0/1 (0)	0/6 (0)	0/0 (0)
Block Name	0/1 (1)	0/6 (0)	0/0 (0)
Beam Meterset	0/394 (368)	**3/422 (69)**	**6/417 (7)**
Number of Control Points	0/394 (0)	0/422 (0)	0/464 (0)
Control Point Index	0/1418 (0)	0/1522 (0)	0/3049 (0)
Control Point Meterset	0/1418 (980)	**3/1522 (163)**	**6/2955 (7)**
Nominal Beam Energy	0/394 (0)	0/422 (0)	0/464 (0)
Dose Rate Set	0/482 (482)[a]	0/422 (422)[a]	**5/464 (5)**
Wedge Position	0/421 (176)	0/565 (0)	0/89 (0)
X Jaws	0/873 (710)	0/863 (0)	**2/464 (2)**
Y Jaws	0/873 (166)	0/863 (0)	0/464 (0)
MLC	**4/862 (862)**	0/842 (0)	**4/2605 (4)**
Gantry Angle	0/394 (0)	0/422 (0)	0/464 (0)
Gantry Rotation Direction	0/394 (0)	0/422 (0)	0/464 (0)
Beam Limiting Device Angle	**1/394 (1)**	0/422 (0)	0/464 (0)
Beam Limiting Device Rotation Direction	0/394 (0)	0/422 (0)	0/464 (0)
Patient Support Angle	**5/394 (5)**	0/422 (0)	0/464 (0)
Patient Support Rotation Direction	0/394 (0)	0/422 (0)	0/464 (0)
Table Top Eccentric Angle	0/394 (0)	0/422 (0)	0/464 (0)
Table Top Eccentric Rotation Direction	0/394 (0)	0/422 (0)	0/464 (0)
Table Top Vertical Position	0/97 (97)[a]	0/399 (399)[a]	0/464 (464)[a]
Table Top Longitudinal Position	0/97 (97)[a]	0/398 (398)[a]	0/464 (464)[a]
Table Top Lateral Position	0/97 (97)[a]	0/399 (399)[a]	0/464 (464)[a]
Number of beams	0/100 (0)	0/100 (0)	0/100 (0)
Number of fractions planned	**29/100 (29)**	**30/100 (30)**	**12/100 (12)**
Total	115/16058 (4699)	58/17930 (2086)	35/21920 (1429)

[a] Parameter excluded from the second step of the analysis.

systems. The highest level of integrity was observed for the system combination Eclipse → Aria which shares a single database (Table 2).

The discrepancies from the second step of the analysis can be classified into seven different categories based on how they occurred (Table 3). Only two types of discrepancies were found for more than one system combination; treatment unit breakdowns and maintenance, affecting the *Number of fractions planned*, and adaptation of treatment, affecting collimator positions and the metersets.

Table 2
Number of discrepancies per beam, identified in the first step of the analysis.

System combination	Number of discrepancies (per beam)
MasterPlan → Visir	11.9
MasterPlan → Aria	4.9
Eclipse → Aria	3.1

Discussion

Block data were found to be associated with a high probability of integrity issues. This information consists of two main parts. One part is associated with the block tray and one part with the block itself. It is not clear in the DICOM standard how this information should be separated. Identification data for the block itself were not available at the planning stage but entered directly in the RV. Most of the block identification data were excluded from the second step in the analysis. Compensators were not utilized at the institution and the attributes related to these types of treatments were expected to be missing.

A detailed analysis of the 208 discrepancies observed in step two was carried out. None of these discrepancies arose in the physical transmission of the data (e.g. due to network failures), but were related to clinical procedures and system designs.

In around 1/4 of all treatment plans the number of fractions changed after treatment planning. This originated from treatment unit breakdowns and scheduled services when the patient was replanned for another treatment unit. If dosimetrically matched treatment units had been available, these issues could have been avoided by allowing the same plan to be treated at another unit. Otherwise, the number of fractions in the TPS must be updated

Please cite this article in press as: Nordström F et al. Ensuring the integrity of treatment parameters throughout the radiotherapy process. Radiother Oncol (2012), doi:10.1016/j.radonc.2012.01.004

Table 3
Number of plans with discrepancies per category, identified in the second step of the analysis. One hundred plans were analyzed for each system combination.

Category	MasterPlan → Visir	MasterPlan → Aria	Eclipse → Aria	All
Treatment unit breakdowns and maintenance	29	34	12	75
Manual editing of data during normal circumstances	21	0	0	21
Acquisition of treatment parameters	5	0	0	5
Information lost during data transfer	0	3	0	3
Correction of errors in treatment plan	0	0	3	3
Adaptation of treatment plan	0	1	1	2
Non-linear chain of data transfer	1	0	0	1
Total	56	38	15	110

with the new number of fractions for the original plan (which depends on the downtime of the unit) in order to maintain a correct treatment record. In parallel, the number of fractions planned for the secondary plan needs to be managed. This highlights the importance of an RV system that can record absorbed doses on a treatment course level and not only on a plan level, and allows treatment course specific dose limits to be defined. Both Visir and Aria have this possibility, which improves the patient safety, but stringent methods are also needed for dealing with these types of hazardous events. This also holds for other types of mid-stream events, requiring data to be altered (e.g. adaptation of the treatment).

All discrepancies in *Beam Meterset* and *Control Point Meterset* originated from manual editing of the planned number of MUs. In all cases except two, the monitor units were changed in order to correct for machine breakdowns where the treatment delivery could not be completed. In one case, the MUs were changed in order to compensate for a large number of portal images. In the second case, the beam weights were adjusted to allow a dynamic wedge field to be delivered with more than 20 MUs.

Similar discrepancies were found for the IMRT treatment plans as for the conventional 3D-CRT plans. None of the discovered discrepancies had any negative impact on the treatment. However, the recurring deviations highlighted procedures that could be associated with an increased risk.

MasterPlan → Visir

The RV Visir was the oldest system in this study and is end-of-life. This system does not export MLC positions that are outside the beam opening. These leaves also have an impact on the delivered dose to the patient. Today this effect could be modeled in many TPSs and the integrity of these MLC positions might be of importance.

In our specific clinical setting, information regarding the gantry angle was, by some operators, routinely added to the beam name, which in Visir originally consists of the beam number. This caused beam label discrepancies. The manual editing of the beam name is not necessary, as the gantry angle is identified by another parameter. During the migration from Visir to Aria this duplication of information was discontinued, and the integrity was improved. The system design of Aria also allows for beam label editing of approved plans and only a single common beam labeling convention can ensure the integrity of this information.

Two of the MLC discrepancies were caused by manual editing of the MLC beam shape and the other two by manual deletion of the MLC in the RV Visir for beams where the beam shape was only defined by the collimator jaws. Manual alignment of individual MLC-leaves might be required in Visir, due to different definitions of valid positions in the two systems. Manual alignment of leaves is undoubtedly a hazardous step and great care must be taken when editing the MLC shape. Further, it was found that the MLC positions are truncated to one decimal during the import from the TPS. When MLC positions are edited in Visir, a rounding toward nearest integer is automatically performed for all MLC positions of the field. The integrity control tool proposed was found to be very useful in the investigation of rounding methods of numerical values within the systems.

The *Beam Limiting Device Angle* (collimator angle) discrepancy arose from a non-linear chain of data transfer. The plan originated from a virtual simulation software (Advantage SIM, GE Healthcare) from which it was transfered both to the RV and the TPS. The number of MUs was calculated in the TPS after a change of the collimator angle from 1° to 0°. The MUs as calculated by the TPS were manually transfered to the RV, but the collimator angle was not updated. This event illustrates the usefulness of the independent integrity check in an environment with a non-linear chain of data transfers, where maintaining data integrity is a much more complex task.

Acquisition of table position during the first treatment in the treatment course caused the table angle discrepancies. A misplacement during this treatment may result in the whole course being delivered with erroneous parameters. In this case the actual table angle was within the RV tolerance (1°) when the table parameters were acquired. The procedure of table parameter acquisition is clearly defined in documented clinical routines, which was followed. However, this acquisition is associated with an increased risk which would have been reduced if only lateral, horizontal and vertical table positions were acquired which is possible in the RV Aria.

MasterPlan → Aria

Bolus information was found to be lost during the data transfer from TPS MasterPlan to RV Aria. This was caused by the fact that only the DICOM-RT Plan file was transfered, but not the DICOM-RT Struct. Bolus is an accessory identified and described mainly by setup notes. However, ensuring the same number of boli is registered in the TPS and RV would provide additional safety.

Eclipse → Aria

The discrepancies in MLC and jaw positions between Eclipse and Aria were, for two beams, caused by an extension of the beams in order to compensate for swelling of the treated volume. For two other beams, MLC leaves outside the beam opening were aligned to the collimators or closed in the Aria system.

The dose rate was changed for one plan in the RV during a transition period, after the clinic decided to move from 500 to 600 MU/min for all 3D-CRT plans.

Design of a data transfer QA program

The proposed method and systematic comparisons between data in the TPS and RV can constitute an important part of a data transfer QA program. However, there are still some parts of such

Please cite this article in press as: Nordström F et al. Ensuring the integrity of treatment parameters throughout the radiotherapy process. Radiother Oncol (2012), doi:10.1016/j.radonc.2012.01.004

a program that are not covered in this study, e.g. to ensure that the approved plan is what the physician intended. If data are cached in an intermediate state, it is also critical that the information on the client side is correctly propagated back to the database. Ideally, the export of data for the comparisons should be performed at a known good database state. The developed software could also be expanded to incorporate logical consistency tests (e.g. IMRT treatment plans must have an MLC), which could prevent accidents such as the one at St. Vincent's Hospital in New York in 2005 [18]. Other examples of logical consistency tests can be found in the literature [14,19]. While the method proposed can be automated in a clinical setting, we and others encourage a final review of the results from these types of integrity checks [14].

Conclusions

The proposed method can be used to verify the integrity of datasets in radiotherapy. This increases the safety for the individual patient by ensuring that the intended treatment is delivered. Treatment unit breakdowns and maintenance, affecting the number of fractions planned, were found to be the most common cause of compromised data integrity. Differences between different system combinations were identified with respect to their ability to maintain data integrity. The system combination providing the highest level of data integrity was found to be one which shares a single database. Some treatment devices, such as blocks and boli were found to be associated with a high probability of compromised integrity. Hazard analysis of the discovered discrepancies can be utilized to identify safety critical procedures and systematic deviations that are associated with an increased risk.

Conflict of interest

The authors declare that there is no conflict of interest.

Acknowledgements

This study was financially supported by the Swedish Cancer Society, The Cancer Foundation at Skåne University Hospital in Malmö and the Cancer Research Foundation at the Department of Oncology, Malmö University Hospital.

Appendix A. Supplementary data

Supplementary data associated with this article can be found, in the online version, at doi:10.1016/j.radonc.2012.01.004.

References

[1] National Electrical Manufacturers Association (NEMA). Digital Imaging and Communications in Medicine (DICOM). Rosslyn: NEMA; 2011. Available from: <ftp://medical.nema.org/medical/dicom/2011 [accessed 09.12.11].
[2] Law MYY, Liu B. Informatics in radiology: DICOM-RT and its utilization in radiation therapy. Radiographics 2009;29:655–67.
[3] Abdel-Wahab M, Rengan R, Curran B, Swerdloff S, Miettinen M, Field C, et al. Integrating the healthcare enterprise in radiation oncology plug and play – the future of radiation oncology? Int J Radiat Oncol Biol Phys 2010;76:333–6.
[4] Clark BG, Brown RJ, Ploquin JL, Kind AL, Grimard L. The management of radiation treatment error through incident learning. Radiother Oncol 2010;95:344–9.
[5] Holmberg O, McClean B. Preventing treatment errors in radiotherapy by identifying and evaluating near misses and actual incidents. J Radiother Pract 2002;3:13–26.
[6] Cunningham J, Coffey M, Knöös T, Holmberg O. Radiation Oncology Safety Information System (ROSIS) – profiles of participants and the first 1074 incident reports. Radiother Oncol 2010;97:601–7.
[7] Swerdloff SJ. Data handling in radiation therapy in the age of image-guided radiation therapy. Semin Radiat Oncol 2007;17:287–92.
[8] Leunens G, Verstraete J, den Bogaert WV, Dam JV, Dutreix A, van der Schueren E. Human errors in data transfer during the preparation and delivery of radiation treatment affecting the final result: garbage in, garbage out. Radiother Oncol 1992;23:217–22.
[9] World Health Organization (WHO). Radiotherapy risk profile – technical manual. WHO: Geneva; 2008. Available from: <http://www.who.int/patientsafety/activities/technical/radiotherapy_risk_profile.pdf> [accessed 09.10.11].
[10] Shafiq J, Barton M, Noble D, Lemer C, Donaldson LJ. An international review of patient safety measures in radiotherapy practice. Radiother Oncol 2009;92:15–21.
[11] Koopman P. 32-bit cyclic redundancy codes for internet applications. In: Proc. int. conf. dependable systems and networks DSN 2002; 2002. p. 459–68.
[12] Knöös T, Johnsson SA, Ceberg CP, Tomaszewicz A, Nilsson P. Independent checking of the delivered dose for high-energy X-rays using a hand-held PC. Radiother Oncol 2001;58:201–8.
[13] Siochi RA, Balter P, Bloch CD, Santanam L, Blodgett K, Curran BH, et al. A rapid communication from the AAPM Task Group 201: recommendations for the QA of external beam radiotherapy data transfer. AAPM TG 201: quality assurance of external beam radiotherapy data transfer. J Appl Clin Med Phys 2011;12:170–81.
[14] Siochi RA, Pennington EC, Waldron TJ, Bayouth JE. Radiation therapy plan checks in a paperless clinic. J Appl Clin Med Phys 2009;10:43–62.
[15] International Electrotechnical Commission (IEC). Medical electrical equipment – requirements for the safety of radiotherapy treatment planning systems. IEC Report 62083. IEC: Geneva; 2000.
[16] International Electrotechnical Commission (IEC). Medical electrical equipment – safety of radiotherapy record and verify systems. IEC Report 62274. IEC: Geneva; 2005.
[17] Riddle WR, Pickens DR. Extracting data from a DICOM file. Med Phys 2005;32:1537–41.
[18] New York State Department of Health. LINAC/IMRT Significant misadministration – software error suspected (Notice No. BERP 2005-1). New York: New York State Department of Health; 2005. Available from: <http://www.health.ny.gov/environmental/radiological/radon/radioactive_material_licensing/docs/berp2005_1.pdf> [accessed 09.12.11].
[19] Furhang EE, Dolan J, Sillanpaa JK, Harrison LB. Automating the initial physics chart checking process. J Appl Clin Med Phys 2009;10:129–35.

Paper II

Radiotherapy and Oncology 102 (2012) 364–370

Contents lists available at SciVerse ScienceDirect

Radiotherapy and Oncology

journal homepage: www.thegreenjournal.com

Quality assurance

Control chart analysis of data from a multicenter monitor unit verification study

Fredrik Nordström [a,*], Sacha af Wetterstedt [b], Stefan Johnsson [c], Crister Ceberg [d], Sven Å.J. Bäck [a,b]

[a] Department of Medical Radiation Physics, Lund University, Malmö, Sweden; [b] Department of Radiation Physics, Skåne University Hospital, Malmö, Sweden; [c] Department of Radiation Physics, Kalmar County Hospital, Sweden; [d] Department of Medical Radiation Physics, Lund University, Lund, Sweden

ARTICLE INFO

Article history:
Received 18 May 2011
Received in revised form 10 November 2011
Accepted 28 November 2011
Available online 10 January 2012

Keywords:
Statistical process control
Control charts
Independent dose calculation
Monitor unit verification

ABSTRACT

Background and purpose: This study aims to investigate the process of monitor unit verification using control charts. Control charts is a key tool within statistical process control (SPC), through which process characteristics can be visualized, usually chronologically with statistically determined limits.

Material and methods: Our group has developed a monitor unit verification software that has been adopted at several Swedish institutions for pre-treatment verification of radiotherapy treatments. Deviations between point dose calculations using the treatment planning systems and using the independent monitor unit verification software from 9219 treatment plans and five different institutions were included in this multicenter study. The process of monitor unit verification was divided into subprocesses. Each subprocess was analyzed using probability plots and control charts.

Results: Differences in control chart parameters for the investigated subprocesses were found between different treatment sites and different institutions, as well as between different treatment techniques. 19 of 37 subprocesses met the clinical specification (±5%), i.e. process capability index was equal to or above one.

Conclusions: Control charts were found to be a useful tool for continuous analysis of data from the monitor unit verification software for patient specific quality control, as well as for comparisons between different institutions and treatment sites. The derived control chart limits were in agreement with AAPM TG114 guidelines on action levels.

In the process of patient specific quality assurance (QA) of radiotherapy plans, monitor unit (MU) verification is considered a central part [1,2]. Several serious incidents in the past could potentially have been prevented if a secondary independent MU calculation had been performed [3–5]. A secondary calculation has for many years been proven to be an efficient tool for prevention of major treatment errors and is important for the patient safety [6]. The calculation method used for verification of the number of MUs required to deliver the prescribed dose to the patient should be independent from that of the primary treatment planning system (TPS). Ideally, independent refers both to the data utilized to characterize the treatment unit, the implementation of the calculation algorithms, as well as the derivation of geometrical data (source-to-surface distance, depth and radiological path length) from the patient anatomy. Several calculation methods have been proposed for the purpose of MU verification [7–10]. Our group has developed a MU verification software (Radiotherapy Verification Program, RVP) that has been adopted at several Swedish institutions for pre-treatment verification of three-dimensional conformal radiotherapy (3D-CRT) treatments. This has enabled a multicenter comparison, as well as statistical analyses on a large collection of data.

It is necessary to define relevant action levels for deviations between the primary and secondary calculation. The accuracy of the two calculation methods in clinically relevant situations forms the basis for these action levels [5]. Clinical implementation of MU verification software usually includes only a single tolerance level for dose or MUs, rather than a complete set of tools for evaluation of calculation results. Statistical process control (SPC) is the application of statistical techniques in order to monitor and improve processes. The benefit of using SPC is that it allows for a quantifiable, numerical analysis of process variability with an emphasis on early detection and prevention of problems. The variation in data can be of two fundamentally different types. Common cause variations are random fluctuations which are expected to be present in any set of measurements. A process that is said to be subjected only to common cause variations are in a state of statistical control. Such a process is stable and predictable. Special cause variations arise from unpredictable, non-random events beyond the expected variability [11]. SPC analysis can be divided into understanding the process, determining the cause of its variability and elimination of the source of special cause variations when they appear. In order to understand a process, it is usually mapped out and monitored using control charts. Control charts is a key concept in SPC and

* Corresponding author.
E-mail address: Fredrik.Nordstrom@med.lu.se (F. Nordström).

0167-8140/$ - see front matter © 2011 Elsevier Ireland Ltd. All rights reserved.
doi:10.1016/j.radonc.2011.11.016

often referred to as one of seven basic quality tools, along with flow (run) charts, cause-and-effect (Ishikawa) diagrams, checklists, pareto charts, histograms and scattergrams. Control charts are used to distinguish between common cause variations and special cause variations. A point falling outside the control chart limits is an indication of a special cause variation, but could also be a false alarm.

A classical approach to characterize a process is to use the mean and standard deviation of the sampled data. However, this does not permit monitoring of the stability of the process variability, while SPC does. The difference between the use of control chart limits and limits calculated from the standard deviation of the same group of data has been illustrated within the field of radiotherapy [12].

Pawlicki et al. have given some examples of SPC applications within radiotherapy QA [12–14]. The process of patient specific IMRT quality control (QC) measurements has been compared to the process of independent dose calculations using control charts [15]. Other investigators have also studied the process of patient specific IMRT QC measurements [16]. Recently, control charts have also been proposed for monitoring the electron spectra from linear accelerators [17].

In contrast to earlier publications this work focuses on the application of control charts on large multicenter data collection and independent 3D-CRT dose calculation verifications. The methodology and conclusions from this work can provide a guideline for implementation of control charts for analysis of results from independent monitor unit verification calculations in combination with other recommendations (e.g. ESTRO [8] and TG114 [5]).

This study aims to investigate deviations between calculations in a software for independent MU verification and the primary TPS using control charts. The process of MU verification was divided into subprocesses which were compared, e.g. corresponding processes at the different institutions participating in this study.

Material and methods

Radiotherapy verification program

Two factor based MU calculation models were implemented into a Microsoft Windows application named Radiotherapy Verification Program, abbreviated RVP (Fig. 1). The first method incorporates an expression for the linear attenuation of the primary photons and an expression for the ratio of scatter-to-primary (SPR) photons (Appendix A). The second method is based on percentage depth dose (PDD) tables and output ratios in water for different field sizes and a single reference source-surface distance (SSD). The Mayneord factor is applied to correct for differences in SSD [18]. For arbitrarily shaped beams, the equivalent field side is determined by solving (A.4) using same parameters as for the SPR model.

The application is written entirely in Microsoft Visual C#.NET using object-oriented programing. Modern treatment planning and record-and-verify systems support the global information-technology standard Digital Imaging and Communications in Medicine (DICOM). A DICOM library was developed and integrated into RVP in order to allow efficient import of all relevant treatment parameters and digital reconstructed radiographs (DRR) generated in the TPS. The user manually selects the location of the calculation point, which ideally complies with ICRU recommendations for prescribing and reporting absorbed dose [19,20]. Heterogeneities inside the patient are taken into account by manually entering the length of bulk density tissues along the beam path to the calculation point. The patient geometry is simplified into a slab geometry based on the SSD, depth, and radiological path-length. The calculation results are displayed as the deviation from the TPS calculated points dose for the individual fields as well as the total plan deviation. Only the latter was investigated in this study and a $\pm 4\%$ action level, based on previous experience with the SPR calculation model [21], was used at all institutions during the data collection period. The PDD-based calculation model in RVP was only used at Institution 3. However, they adopted the same action level for their independent dose calculations as the other institutions.

This study includes 12 linear accelerators (Elekta and Varian Medical Systems). The primary dose calculations were performed using the Pencil Beam Convolution (PBC) algorithm in either Eclipse (Varian Medical Systems) or MasterPlan (Nucletron) or using the Anisotropic Analytical Algorithm (AAA) in Eclipse. Deviations between point dose calculations in TPS and in RVP for 9219 treatment plans from five different institutions were analyzed.

Statistical process control

There are several different types of control charts available within SPC and selecting an appropriate one can be a difficult task. Flow charts, based on the data to be plotted and the format in which the data are collected, can aid this decision [11]. The data analyzed in this study were individual calculation results and the use of the Shewhart individuals control chart (individual/moving-range chart or XmR chart) was therefore appropriate. All data points were arranged in chronological order. Process capability analysis was also performed in order to determine and compare the subprocesses' ability to generate results within specification.

Shewhart individuals control chart

The XmR chart concept contains two types of charts; one that displays the individual measured values (X chart) and one that displays the difference from one measurement to the next (mR chart). The moving range (mR_i) is determined by (1), where x_i represents a single dose difference calculation. $\overline{mR}$ is the average moving range between successive dose difference calculations (2) and hence a measure of the dispersion of the data. This constitutes the centerline of the mR chart. The number of dose difference calculations is denoted n.

$$mR_i = |x_i - x_{i-1}| \tag{1}$$

$$\overline{mR} = \frac{\sum_{i=2}^{n} mR_i}{n-1} \tag{2}$$

The upper control chart limit (UCL) for the mR chart was calculated using:

$$UCL = D_4 \cdot \overline{mR} = 3.267 \cdot \overline{mR} \tag{3}$$

Upper and lower control chart limits for the X charts were calculated using (4) and (5), where $\bar{x}$ is the average difference between TPS and RVP (center line) over n number of calculations.

$$UCL = \bar{x} + \frac{3 \cdot \overline{mR}}{D_2} = \bar{x} + 2.66 \cdot \overline{mR} \tag{4}$$

$$LCL = \bar{x} - \frac{3 \cdot \overline{mR}}{D_2} = \bar{x} - 2.66 \cdot \overline{mR} \tag{5}$$

The constants D_2 and D_4 are anti-biasing constants and the values of these can be found in textbooks [22]. The constant 3 has traditionally been used as a trade-off between the sensitivity of the control chart and the resources available to determine the cause of data points falling outside the limits [23].

As a rule of thumb, 25 data points have been recommended as a minimum for calculation of control chart limits [23]. Using a small number of initial data points for calculating the limits could be beneficial for processes with low throughput, as it otherwise would take a long time before they could be monitored. However,

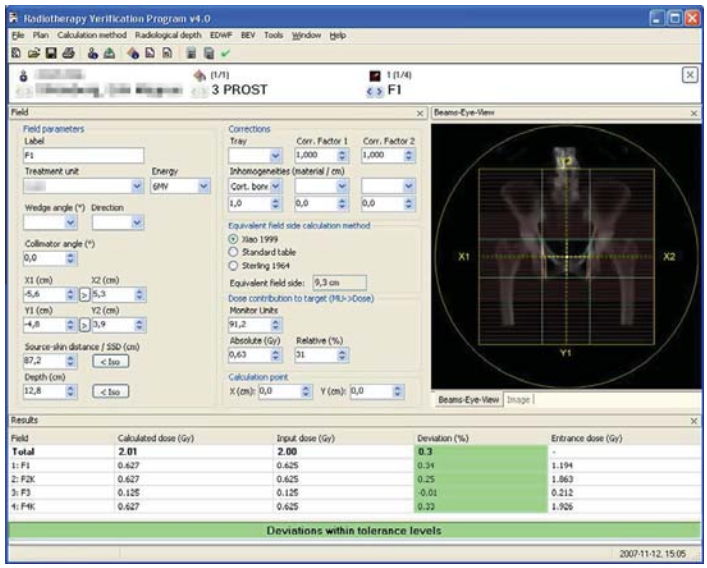

Fig. 1. The user interface of RVP.

the uncertainty in the computed limits will decrease as the amount of data used to compute the limits increases. As a balance between the accuracy in the computed control chart limits and the number of plans needed to begin the monitoring process, the 50 initial plans in each subprocess were used for calculation of the control chart limits in this study.

Process capability

The process capability index determines if a process is able to meet its specification. The specification limit is a statement of the user requirement and has no connection to the control chart limit, which is estimated from the data. A specification level of 5% absorbed dose difference was chosen after considering the combined uncertainty between RVP and TPS, as well as the overall accuracy requirements of 2.5–3.5% (1 s.d.) [24–27]. A 5% level has also been proposed as a guideline for action levels for disagreement between verification and primary calculations for the more complex 3D-CRT treatments, involving low density heterogeneities and small fields [5]. The 5% level was also used in previous works by Pawlicki et al. [12,15]. The capability index is calculated using (6) for normal distributed data. *USL* and *LSL* are the upper and lower specification limits (±5%), respectively. $\bar{x}$ and s are estimates of the mean and the standard deviation of the process, respectively.

$$\widehat{C}_{pk} = min\left[\frac{USL-\bar{x}}{3s}, \frac{\bar{x}-LSL}{3s}\right] \quad (6)$$

When the process distribution is not normal, another set of indices that apply to non-normal distributions could be used [16,28]. The non-parametric capability index is estimated by

$$\widehat{C}_{npk} = min\left[\frac{USL-median}{p(0.995)-median}, \frac{median-LSL}{median-p(0.005)}\right] \quad (7)$$

where $p(0.995)$ is the 99.5th percentile of the data and $p(0.005)$ is the 0.5th percentile of the data. The capability indices were calculated using all data points for each subprocess, except for outliers in the initial data (see Section 'Data characterization').

Data characterization

Subprocesses were identified from the stored treatment plan parameters (e.g. institution, treatment unit, treatment site, signature/operator, and number of beams) and then used to group the data. The parameters that resulted in subprocesses with a large change from the main process in $\widehat{C}_{pk}$ and mean value were considered to be the most important. Further, the number of data points in each subprocess was taken into account. Mean value and process capability index were only calculated for subprocesses with more than 50 data points.

Normal probability plots were generated in order to verify the assumption of approximately normally distributed data. In case of a normal distribution, the data plotted should form an straight line that corresponds to a theoretical normal distribution. Additionally, an Anderson–Darling normality test ($\alpha = 0.05$) was performed.

The data set contained some large deviations (>15%) that would have a strong impact on the analysis if they were not excluded. The deviations typically originated from single beams being verified and therefore the total deviation, as calculated by RVP, was not valid. These outliers were identified using Rosner's test ($\alpha = 0.01$) and excluded if they did not indicate actual special cause deviations.

Results and discussion

Data characterization

A differentiation into institutions, treatment sites and treatment techniques was found to derive the most meaningful subprocesses for the purpose of generating control charts. The 66 resulting subprocesses derived from the combination of these

three parameters had a relatively high throughput with regard to the number of plans verified during the data collection period (67 in median). Out of the 66 subprocesses, 37 had more than 50 plans and were further analyzed. These subprocesses had a wide range in the numerical values of the SPC parameters (e.g. center line, control chart limits and process capability, see Section 'Control charts'). Subprocesses derived from the institution parameter in combination with treatment site and technique can be utilized until sufficient amount of data has been acquired to allow the addition of the treatment unit parameter, generating more narrow subprocesses. The user signature parameter resulted in subprocesses with a median of only 10 plans, which was not considered enough for meaningful control chart analysis. A differentiation based on the number of beams parameter had only a minor impact on the process capability index (ranging between 1.21 and 1.36) and was therefore not used.

It is clear that different treatment sites and treatment techniques result in different deviation distributions. A differentiation based on these parameters is therefore valuable in order to increase the process capability by reducing the moving range of the data. These findings are in agreement with a previous study [29]. Other investigators have also suggested that the action limits should be specific to treatment site and technique [5,29]. Examples of treatment techniques include intensity-modulated radiotherapy (IMRT), volumetric arc-therapy (VMAT), stereotactic radiotherapy (SRT) and three-dimensional conformal radiotherapy (3D-CRT).

The Anderson–Darling test resulted in the zero-hypothesis of normally distributed data to be rejected at a 5% level for 25 of the 37 subprocesses. However, the generated probability plots verified the assumption of approximately normally distributed data (Fig. 2).

The subprocesses derived from the breast treatment site parameter were among the most non-normally distributed data. This can have several explanations, e.g. small or narrow fields, not accounting for missing phantom scatter outside the patient contour in RVP and large variations in phantom scatter conditions.

A clear change in probability around ±4%, which has constituted the traditional action level, can be observed (Fig. 2). This is caused by the method used to correct for heterogeneities. Investigations have shown that the users do not always correct for heterogeneities if the deviation is within the action limits. For deviations outside the action limits, the users tend to "tweak" the bulk densities until the deviation is within tolerance. An independent ray-tracing in order to calculate the SSD and the radiological path-length would be preferable, avoiding the uncertainty associated with the manual input.

Control charts

Control chart analysis was performed on the 37 subprocesses using 50 initial plans to calculate the control chart limits and center lines. 39 of 8759 plans were excluded from the analysis, by applying Rosner's test for outliers ($\alpha = 0.01$) on each individual subprocess. None of the excluded data points indicated actual special cause deviations. Only data from RVP were analyzed in this study, but the concept of control charts and subprocesses could be valid for other MU verification software as well.

Center line values ranged between −1.7% and 1.6% and the half width of the limits between 1.8% and 6.8% for the subprocesses. The half width of the limits are in good agreement with the guidelines for action levels proposed by AAPM report TG114 on verification of monitor unit calculations (Table 1) [5]. Control charts could

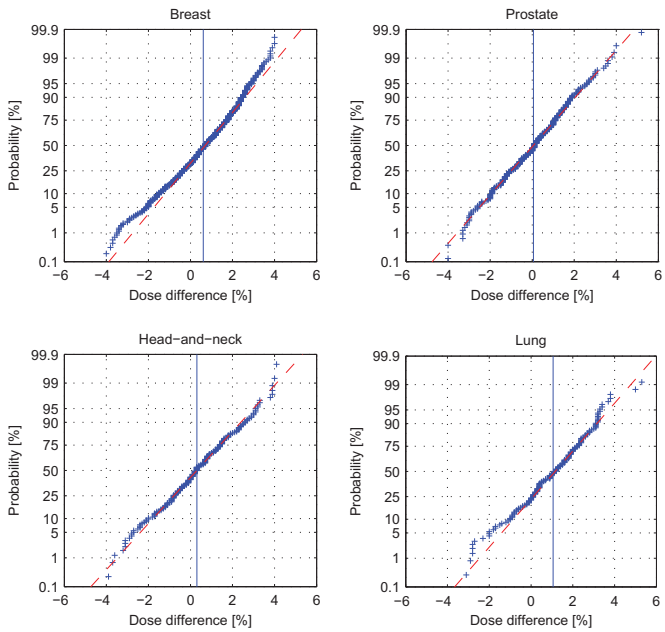

Fig. 2. Normal probability plots for four different treatment sites at Institution 2 using 3D-CRT technique. The straight red line corresponds to a theoretical normal probability distribution for each data set. The blue lines are the mean dose differences of the data sets.

Table 1
Comparison between TG114 action levels and the half width of the control chart limits averaged over all institutions. The values from TG114 were selected based on the calculation geometry characteristics, the use of different calculation algorithms and "approximate patient" geometry.

Case	TG114 (%)	Control chart (%)
Brain	3[a]	2.7
Breast	4[b]	4.0
Large field lung	5[c]	4.3
Small field lung	5[c]	4.2

[a] Homogeneous conditions, minimal field shaping.
[b] Homogeneous conditions, wedged fields, off-axis.
[c] Small fields and/or low-density heterogeneity.

provide an efficient way of deriving action levels for use in conjunction with the recommendations from TG114. However, the use of control charts should not replace a comprehensive commissioning of neither the monitor unit verification software nor the primary TPS.

For non-normally distributed data, the estimate of the non-parametric capability index (7) would usually be preferable. However, due to the software's functionality, allowing the user to "tweak" the bulk densities in order to achieve results within the action levels, many percentile values were accumulated around ±4%. A subprocess with a median value near zero, will then always have a capability index around 1.25. This was found to be the case for many of the subprocesses. Based on these findings, the capability index C_{pk} was instead used for all subprocesses. This index is proportional to the distance between the control chart limits and the center line. Therefore, a non zero centerline would reduce the process capability. Further, a larger distance between the control charts limits would usually reduce the process capability, due to an increased standard deviation estimate.

32 of 37 subprocesses were found to be in statistical control after analyzing the initial 50 calculation points used for generating the control chart limits. The process capability indices ranged between 0.7 and 1.7 for these subprocesses. 19 subprocesses met the clinical specification (±5%), i.e. capability index was equal to or above one. However, 27 of the subprocesses would be within the clinical specification if it was changed to 6%. A more detailed compilation for 20 of the subprocesses (5 institutions and 4 treatment sites using 3D-CRT technique) is presented in Table 2. The total percentage of calculations outside the control chart limits was 2.1% for the subprocesses analyzed and major differences (0.0–10.3%) between subprocesses were identified. The higher percentage was observed for subprocesses with small limit half width, due to very similar patient geometries and beam settings. However, the data also contained a few plans associated with a completely different beam setting and geometry which therefore had a high probability to fall outside the limits. These plans should have been placed in another subprocess.

Differences in control chart parameters for the investigated subprocesses were found between different treatment sites and institutions, as well as between different treatment techniques.

Treatments of the breast using asymmetric technique constitute processes with low capability indices (ranging between 0.72 and 0.92) at all the institutions. These subprocesses include plans with relatively high complexity, e.g. with calculations at off-axis points near field edges in heterogeneous volumes. Subprocesses where it is possible to select the calculation point so that it fulfills the recommendations from ICRU for prescribing and reporting absorbed dose (i.e. points where transient electron equilibrium is established), result in smaller width between the control chart limits and a higher process capability. The half width of the limits from Institution 3 were considerably lower compared to those of similar processes at other institutions. This originated from the PDD-table based calculation method used for the independent dose calculation at this institution. Especially for heterogeneous volumes, this method produced results with smaller moving range compared to the SPR method used at the other institutions. Differences in control chart parameters were also observed between institutions using the same types of TPS:s and accelerators. For some treatment sites, especially in heterogeneous volumes, clinics with higher moving range and lower process capabilities also had a larger variation between users (i.e. signatures). Some users also had a larger variation in their calculation results compared to their institution colleagues. This indicates that the difference did not arise from the beam data in TPS or RVP, but in how stringent the methodology for monitor unit verification is at that institution. By reducing the flexibility in the software, e.g. by introducing non-user associated determination of geometrical parameters and the use of well defined methodology for the process, these user variations could be minimized. Other quality assurance processes (e.g. IMRT verification measurements) are likely to exhibit similar user variations.

One of the strengths with control charts is that the data is processed chronologically. At one institution, a migration from using the PBC algorithm in MasterPlan to the AAA algorithm in Eclipse was undertaken during the data collection period. The effect of this can be seen as an increase in the mean value after 156 calculated plans, while the average moving range remains on a similar level

Table 2
Control chart parameters for 16 of the total 37 analyzed subprocesses, including 5 different institutions and 4 different treatment sites for the 3D-CRT treatment technique. Process capability indices was not calculated for processes that were determined to be out of control after the initial 50 plans had been analyzed.

Treatment site	Institution 1	Institution 2	Institution 3	Institution 4	Institution 5
X-chart center line (%)					
Breast	0.99	0.06	0.81	−0.74	0.57
Prostate	1.60	0.35	0.65	1.34	1.14
Head and neck	0.47	0.51	–	–	1.32
Lung	−0.38	1.52	0.28	–	–
X-chart limits half width, $2.66 \cdot \overline{mR}$ *(plans outside limits) (%)*					
Breast	3.49 (3.3)	5.03 (0.0)	3.10 (0.6)	4.04 (0.0)	4.46 (1.1)
Prostate	4.49 (1.7)	3.27 (4.0)	2.12 (0.0)	3.64 (2.8)	3.21 (3.0)
Head and neck	6.02 (0.0)	4.25 (0.5)	–	–	5.01 (0.0)
Lung	5.46 (0.0)	4.64 (0.6)	2.80 (4.5)	–	–
Process capability index, C_{pk} *(total number of plans)*					
Breast	N/A (484)	0.96 (755)	1.23 (166)	0.89 (161)	0.97 (175)
Prostate	N/A (458)	N/A (377)	1.72 (149)	0.95 (326)	N/A (67)
Head and neck	1.01 (419)	0.93 (210)	– (10)	– (22)	0.70 (50)
Lung	0.82 (218)	0.80 (178)	1.19 (66)	– (14)	– (30)

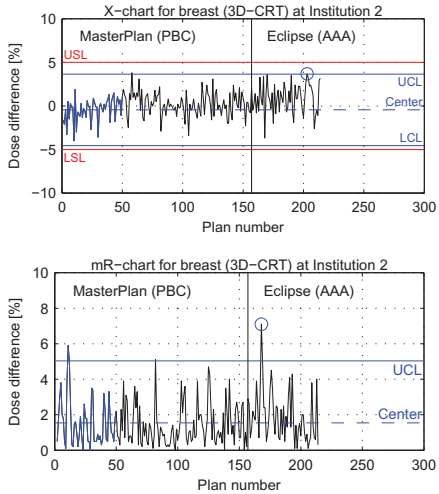

Fig. 3. Control charts for the subprocess derived from the breast treatment site and 3D-CRT treatment technique at a single treatment unit at Institution 2. The PBC algorithm in MasterPlan was used until calculation 157 when the AAA in Eclipse was implemented. The blue data points represent the initial 50 plans used for determination of the control chart limits. The red lines represents the specification level of ±5%.

(Fig. 3). The 11th and the 46th calculation using AAA fell outside the mR-chart limits and the X-chart limits, respectively. Having implemented the use of control charts, the points outside the control chart limits would have triggered an investigation and potentially revealed the effect on the process of MU verification from the migration to AAA and Eclipse. Methods such as histograms would not have been as fast to indicate a change in the processes. After determining and accepting the cause of the change in the process, the modified process should be mapped out and new control chart limits should be calculated.

Conclusion

Control charts were shown to be a useful tool for continuous analysis of data from MU verification software for patient specific quality control. The construction and analysis of the control charts have improved the understanding of the monitor unit verification process from a clinical point of view, as well as allowed for statistically relevant treatment site and technique specific action levels (control chart limits) to be applied. Differences between subprocesses were discovered using X- and mR-charts. Center line and X-chart limit half-width are relevant parameters for comparison of similar processes, e.g. MU verification for different treatment sites and techniques at a specific institution, in order to identify systematic errors and weaknesses. Some differences were related to the user associated flexibility in the process. To minimize the dispersion of the calculation results, stringent methods for MU verification calculations could be employed.

By improving the heterogeneity correction in the SPR model or by using the PDD model, the capability of the process of monitor unit verification using these factor based calculation models could perform within a clinical specification of 5%. The derived X-chart limits were in agreement with TG114 guidelines on action levels.

Conflict of interest statement

The authors declare that there is no conflict of interest.

Acknowledgment

This study was financially supported by the Swedish Cancer Society.

Appendix A. Dose calculation method

The independent calculation model used in this study is factor based. The number of MU calculated by the TPS (M) is used in order to perform an independent calculation the absorbed dose (D) for each field to a point of interest (A.1).

$$D = M \cdot \left(\frac{D}{M}\right)_{ref} \cdot K_p^{rel} \cdot \frac{T}{T_{ref}} \cdot \left(\frac{\beta_P + \sigma}{\beta_{P,ref} + \sigma_{ref}}\right) \tag{A.1}$$

The factor β_P describes the effect of the transport of secondary electrons (i.e. degree of transient electronic equilibrium). The primary kerma 'free in-air' relative (rel) to a reference field (ref), $K_P^{rel} = K_{P,0}/K_{P,0,ref}$ is a function of the collimator equivalent square (c_{eq}) and the distance from the X-ray source (f) and is calculated as a factor between the relative head-scatter factor and the inverse-square law (A.2).

$$K_P^{rel}(c_{eq}, f) = \frac{a_1 + a_2 c_{eq}}{1 + a_3 c_{eq} + a_4 c_{eq}^2} \cdot \left(\frac{f_{ref}}{f}\right)^2 \tag{A.2}$$

The parameters a_1 to a_4 are fitted to measurements at different c_{eq} for $f = f_{ref}$, thus it has been shown that K_P^{rel} is a measurable quantity [30].

The transmission factor (T) that accounts attenuation of the primary photons due to the presence of a medium is a function of the mean linear attenuation coefficient (μ), the beam-hardening coefficient (η) and the radiological path length (z_{rad}) (A.3).

$$T(z) = e^{-\mu \cdot z_{rad}(1 - \eta \cdot z_{rad})} \tag{A.3}$$

The values of μ and η is determined from transmission measurements [30,31]. A semi-empirical formalism, as a function of the equivalent field side s and the depth z, is used to determine the scatter-to-primary kerma ratio σ [31–34] (A.4).

$$\sigma(s, z) = \frac{a \cdot s \cdot z}{w \cdot s + z} \tag{A.4}$$

It has been found that a and w are linear functions of μ [32]. For an arbitrary shaped beam the σ is determined by summing the contributions from a number of right triangles that constitute the field [35]. Physical wedges are handled as separate beam qualities and enhanced dynamic wedges (EDW) are handled using an modification of the fractional MU approximation [36].

The main part of the calculation model in RVP has been described in more detail elsewhere [21,37].

References

[1] Nyholm T. Verification of dose calculations in radiotherapy. Ph.D. thesis; Umeå University; Umeå; 2008. http://urn.kb.se/resolve?urn=urn:nbn:se:umu:diva-1931 [accessed 8 November 2011].
[2] Sellakumar P, Arun C, Sanjay SS, Ramesh SB. Comparison of monitor units calculated by radiotherapy treatment planning system and an independent monitor unit verification software. Phys Med 2011;27:21–9.
[3] Unintended overexposure of patient Lisa Norris during radiotherapy treatment at the Beatson Oncology Centre, Glasgow in January 2006. Report of the investigation by Inspector appointed by the Scottish Ministers for the Ionizing Radiation (Medical Exposures) Regulations. Edinburgh; 2006. http://www.scotland.gov.uk/Publications/2006/10/27084909/0 [accessed 8 November 2011].

[4] Summary of ASN report no. 2006 ENSTR 019 - IGAS no. RM 2007-015P on the Epinal radiotherapy accident, submitted by Guillaume Wack (ASN, the French Nuclear Safety Authority) and Dr. Françoise Lalande, member of the Inspection Générale des Affaires Sociales (General inspectorate of Social Affairs), in association with Marc David Seligman. Paris; 2007. http://www.asn.fr/index.php/content/download/15545/100850/ASN_report_n_2006_ENSTR_019_-_IGAS.pdf [accessed 8 November 2011].
[5] Stern RL, Heaton R, Fraser MW, Goddu SM, Kirby TH, Lam KL, et al. Verification of monitor unit calculations for non-IMRT clinical radiotherapy: report of AAPM Task Group 114. Med Phys 2011;38:504–30.
[6] López PO, Cosset JM, Dunscombe P, Holmberg O, Rosenwald JC, Ashton LP, et al. ICRP publication 112. A report of preventing accidental exposures from new external beam radiation therapy technologies. Ann ICRP 2009;39:1–86.
[7] Kung JH, Chen GTY, Kuchnir FK. A monitor unit verification calculation in intensity modulated radiotherapy as a dosimetry quality assurance. Med Phys 2000;27:2226–30.
[8] Dutreix A, Bjärngard BE, Bridier A, Mijhheer B, Shaw JE, Svensson H. Monitor unit calculation for high energy photon beams, Physics for clinical radiotherapy. ESTRO Booklet No. 3. Leuven: Garant; 1997.
[9] Nyholm T, Olofsson J, Ahnesjö A, Karlsson M. Photon pencil kernel parameterisation based on beam quality index. Radiother Oncol 2006;78:347–51.
[10] Pisaturo O, Moeckli R, Mirimanoff RO, Bochud FO. A Monte Carlo-based procedure for independent monitor unit calculation in IMRT treatment plans. Phys Med Biol 2009;54:4299–310.
[11] Stapenhurst T. Mastering statistical process control. Oxford: Elsevier Butterworth-Heinemann; 2005.
[12] Pawlicki T, Yoo S, Court LE, McMillan SK, Rice RK, Russell JD, et al. Process control analysis of IMRT QA: implications for clinical trials. Phys Med Biol 2008;53:5193–205.
[13] Pawlicki T, Whitaker M, Boyer AL. Statistical process control for radiotherapy quality assurance. Med Phys 2005;32:2777–86.
[14] Pawlicki T, Whitaker M. Variation and control of process behavior. Int J Radiat Oncol Biol Phys 2008;71(1 Suppl):S210–4.
[15] Pawlicki T, Yoo S, Court LE, McMillan SK, Rice RK, Russell JD, et al. Moving from IMRT QA measurements toward independent computer calculations using control charts. Radiother Oncol 2008;89:330–7.
[16] Breen SL, Moseley DJ, Zhang B, Sharpe MB. Statistical process control for IMRT dosimetric verification. Med Phys 2008;35:4417–25.
[17] de la Vega JM, Martínez-Luna RJ, Guirado D, Vilches M, Lallena AM. Statistical control of the spectral quality index in electron beams. Radiother Oncol 2012;102:406–11.
[18] Khan FM. Dose distribution and scatter analysis. In: Khan FM, editor. The physics of radiation therapy. Philadelphia: Lippincott Williams and Wilkins; 2003. p. 159–77.
[19] International Commission on Radiation Units and Measurements (ICRU). Prescribing, recording and reporting photon beam therapy, ICRU report no. 50. Bethesda: ICRU; 1993.
[20] International Commission on Radiation Units and Measurements (ICRU). Prescribing, recording and reporting photon beam therapy, ICRU Report no. 62 (Supplement to ICRU Report 50). Bethesda: ICRU; 1999.
[21] Knöös T, Johnsson SA, Ceberg CP, Tomaszewicz A, Nilsson P. Independent checking of the delivered dose for high-energy X-rays using a hand-held PC. Radiother Oncol 2001;58:201–8.
[22] Montgomery DC. Introduction to statistical quality control. Hoboken: John Wiley & Sons; 1996.
[23] Shewhart W. Economic control of quality of manufactured product. Princeton: D. Van Nostrand Company, Inc.; 1931.
[24] Brahme A. Dosimetric precision requirements in radiation therapy. Acta Radiol Oncol 1984;23:379–91.
[25] Goitein M. Nonstandard deviations. Med Phys 1983;10:709–11.
[26] Mijnheer BJ, Battermann JJ, Wambersie A. What degree of accuracy is required and can be achieved in photon and neutron therapy? Radiother Oncol 1987;8:237–52.
[27] International Atomic Energy Agency (IAEA). Technical reports series no. 398: Absorbed dose determination in external beam radiotherapy - an international code of practice for dosimetry based on standards of absorbed dose to water. Vienna: IAEA; 2000.
[28] Kotz S, Johnson NL. Process capability indices. London: Chapman & Hall; 1993.
[29] Georg D, Nyholm T, Olofsson J, Kjaer-Kristoffersen F, Schnekenburger B, Winkler P, et al. Clinical evaluation of monitor unit software and the application of action levels. Radiother Oncol 2007;85:306–15.
[30] Johnsson SA, Ceberg CP, Knöös T, Nilsson P. Transmission measurements in air using the ESTRO mini-phantom. Phys Med Biol 1999;44:2445–50.
[31] Bjärngard BE, Shackford H. Attenuation in high-energy X-ray beams. Med Phys 1994;21:1069–73.
[32] Bjärngard BE, Vadash P, Ceberg CP. Quality control of measured X-ray beam data. Med Phys 1997;24:1441–4.
[33] Bjärngard BE, Vadash P. Analysis of central-axis doses for high-energy X-rays. Med Phys 1995;22:1191–5.
[34] Bjärngard BE, Zhu TC, Ceberg C. Tissue-phantom ratios from percentage depth doses. Med Phys 1996;23:629–34.
[35] Xiao Y, Bjärngard BE, Reiff J. Equivalent fields and scatter integration for photon fields. Phys Med Biol 1999;44:1053–65.
[36] Kuperman VY. Analytical representation for varian EDW factors at off-center points. Med Phys 2005;32:1256–61.
[37] Johnsson S. Development and evaluation of an independent system for absorbed dose calculations in radiotherapy. Ph.D. thesis; Lund University; 2003. http://www.lub.lu.se/ [accessed 8 November 2011].

Paper III

Since this paper is not yet published it has been removed from the public online version of this thesis. The full version of the thesis is available upon request. Please send an email to Fredrik.Nordstrom@med.lu.se.

Paper IV

Since this paper is not yet published it has been removed from the public online version of this thesis. The full version of the thesis is available upon request. Please send an email to Fredrik.Nordstrom@med.lu.se.

Paper V

Journal of Physics: Conference Series **250** (2010) 012059 doi:10.1088/1742-6596/250/1/012059

3D geometric gel dosimetry verification of intraprostatic fiducial guided hypofractionated radiotherapy of prostate cancer

Fredrik Nordström[1,2], Sofie Ceberg[1,2], Sacha af Wetterstedt[2], Per Nilsson[3,4], Crister Ceberg[5], Sven ÅJ Bäck[1,2]

[1]Department of Medical Radiation Physics, Lund University, Malmö, Sweden

[2]Department of Radiation Physics, Skåne University Hospital, Malmö, Sweden

[3]Department of Radiation Physics, Skåne University Hospital, Lund, Sweden

[4]Department of Radiation Sciences, Umeå University, Umeå, Sweden

[5]Department of Medical Radiation Physics, Lund University, Lund, Sweden

Fredrik.Nordstrom@med.lu.se

Abstract. This pre-study is aimed to investigate the feasibility of a normoxic polyacrylamide gel (nPAG) dosimeter with implanted gold fiducials to evaluate the geometric precision, including setup correction strategies, in the delivery of hypofractionated treatments. For this purpose a phantom consisting of three parts was constructed: (1) the patient simulating volume, providing realistic scatter conditions and weight, (2) a bottle containing the active dosimetric volume and (3) the gold fiducials and the fiducial support structure. A 6.1 Gy prostate IMRT treatment was delivered to the phantom using the sliding-window technique. The phantom was positioned prior to the treatment using the implanted fiducials and kV on-board imaging. An overlay of the 95% isosurface of the TPS calculated dose distribution and the measured dose distribution using gel showed good agreement. The clinical target volume (CTV) was well centred inside the 95% isodose surface of the measured volume. It was shown for the evaluated case that the use of on-board imaging and integrated setup correction tools could be used to compensate for a deliberately introduced offset in CTV position. The study showed that MRI based nPAG gel dosimetry can be used to verify setup correction procedures using implanted gold fiducials.

1. Introduction

Several studies have suggested that dose-escalated external radiotherapy could prolong the freedom from failure time, measured as a rising prostate-specific antigen (PSA) [1-3]. On the other hand, preliminary results from a randomized MD Anderson study reported an increase of rectal toxicity in the dose-escalation arm by a factor of two [4]. If the prostate is localized prior to treatment and by adjusting the patient position to account for the inter-fraction prostate movement, the planning target volume (PTV) could be reduced [5]. This would reduce the dose to the surrounding normal tissue,

including rectum, and potentially reduce side-effects of the treatment. Image guided radiotherapy (IGRT) has been widely adopted to minimize the effects of inter-fractional motion. Intraprostatic gold fiducials are the most wide-spread approach for IGRT of the prostate in clinical practice [6]. The importance of prostate localization is undoubtedly higher when increasing the fraction dose.

A randomized multicenter phase III study (HYPO-RT-PC) of patients with intermediate risk prostate cancer has been initiated [7]. Conventional fractionation (2.0 Gy in 39 fractions) to a total absorbed dose of 78.0 Gy is compared with hypofractionation (6.1 Gy in 7 fractions) to a total absorbed dose of 42.7 Gy. All fractions are delivered with either conventional (3D-CRT) or intensity modulated radiotherapy (IMRT). The position of the prostate, as determined by the implanted gold fiducials, is verified prior to each fraction with kV/MV portal imaging or cone beam CT.

Polymer gel dosimetry can be used to measure absorbed dose distributions in a complete volume with high spatial resolution [8, 9]. The use of gel dosimetry has also been found feasible for verification of dynamic delivery [10, 11].

This pre-study aims to investigate the feasibility of a normoxic polyacrylamide gel (nPAG) dosimeter with implanted gold fiducials to evaluate the dosimetric consequences of the setup correction strategies used at the centers participating in the HYPO-RT-PC study.

2. Material and methods

2.1. Gel preparation

In this study a single batch of normoxic polyacrylamide gel (nPAG) was used, based on 3% w/w acrylamide (electrophoresis grade, ≥99%, powder, Sigma Aldrich) and 3% w/w N,N´-methylenebisacrylamide (electrophoresis grade, ≥98%, powder, Sigma Aldrich). Gelatine (300 bloom, Sigma Aldrich) was used as the matrix substance and tetrakis(hydroxymethyl)–phosphonium chloride (techn. ~80% in water, Sigma Aldrich) was used as an oxygen scavenger. The remaining constituent was ultra-pure deionized water (resistivity > 18.2 MΩ cm). The method used for gel preparation has been described elsewhere [12]. Vials containing the gel were irradiated with an absorbed dose ranging from 1 to 7 Gy in order to assure the linearity of the gel dose response for this batch of gel.

2.2. Phantom

The phantom consists of three parts: the patient simulating volume, providing realistic scatter conditions and weight, a bottle containing the active dosimetric volume and the fiducials and the fiducial support structure (figure 1). The outer part of the phantom was created using polystyrene slabs of 5 mm thickness that were glued together and modified to an oval shape to simulate the body outline in the pelvic region. A hole was drilled in the center of the polystyrene that fits an oxygen resistant glass bottle, containing the nPAG gel. The fiducials (1 mm diameter, 5 mm length) were fixated at the ends of three 5 mm thick polymethyl methacrylate (PMMA) rods attached to the lid of the bottle.

2.3. CT scanning and treatment planning

Treatment planning was performed on planar CT images of the phantom with a slice thickness of 3 mm, in accordance with the HYPO-RT-PC study protocol. Structures from a dummy patient was imported onto the phantom and a six field, 6 MV, sliding-window IMRT treatment plan was created with a fractional dose of 6.1 Gy (figure 1). The planning target volume (PTV) included the prostate (CTV) with a margin of 7 mm in all directions. All DVH constraints and technical aspects of the study protocol were fulfilled. The TPS calculated dose matrix was interpolated from 2.5 × 2.5 × 3 mm to 1 × 1 × 3 mm using cubic spline.

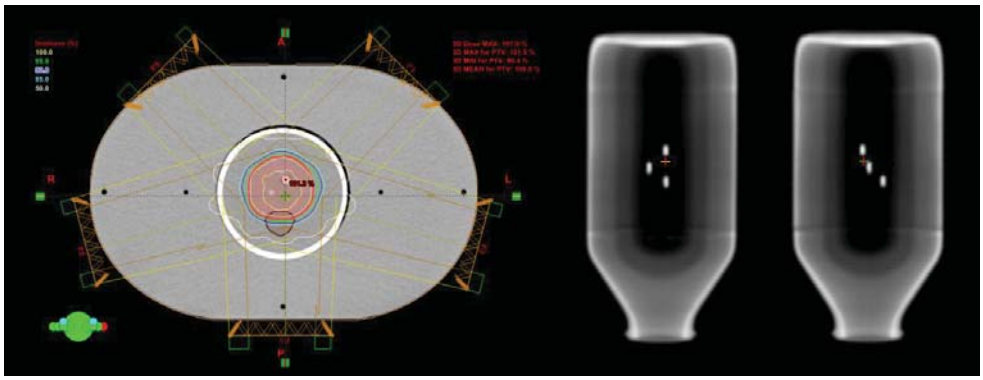

Figure 1. The six field, 6MV, sliding-window IMRT treatment plan with structures from a dummy patient (left). The fiducials are clearly visible in the digital reconstructed radiographs (DRR) generated in 0° and 270°, respectively (middle and right).

2.4. Treatment delivery

A Clinac 2100C/D (Varian medical systems) equipped with an x-ray on-board imager (OBI) was used for treatment delivery. The phantom was intentionally placed at an offset position from iso-center, with a rotation of the glass bottle around the longitudinal axis. Planar imaging at 0° and 270° using the OBI was performed and the integrated automatic correction possibilities (longitudinal, lateral and vertical couch movement) in the Aria verification system (Varian medical systems) were used to correct for the simulated misplacement. The dose-rate was 400 monitor units per minute and Portal Dosimetry (Varian medical systems) was performed prior to the gel dosimetry in order to exclude possible machine-dependent errors.

2.5. Magnetic resonance imaging

Magnetic resonance imaging (MRI) of the gels was carried out 24 hours after the irradiation, using a 1.5 T MRI unit (Siemens Medical Systems) and a circularly polarized receive-only head coil. The images were acquired using a 32-echo multi spin echo sequence with an inter-echo spacing of 25 ms and a repetition time of 4000 ms. The voxel size was 1 × 1 × 3 mm. To obtain an accurate background signal, an unirradiated gel bottle of the same dimensions was also scanned. An in-house developed software was used for calculation of the transversal relaxation rate (R2 = 1 / T2) [13].

3. Results and discussion

The γ pass-ratio between the measured and calculated EPID dose distribution agreed within 96 % using a 3% / 3 mm criterion, confirming that there was no machine dependent delivery errors.

The planar images obtained with the OBI at 0° and 270° were matched with the DRRs generated in the TPS using the Aria (Varian medical systems) verification system, and the resulting geometrical corrections were used to account for the present offset (figure 2, table 1).

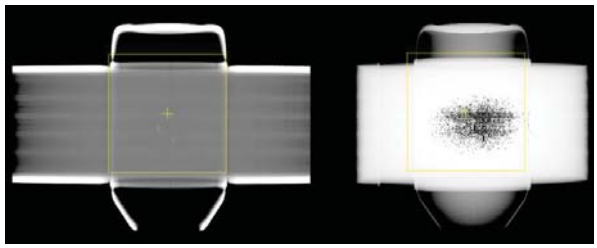

Figure 2. kV images of the phantom taken with the OBI at 0° (left) and 270° (right). The images were matched against the DRR generated in the TPS and used to correct for the offset.

Table 1. Position of the phantom relative to the iso-center determined using an external laser system (LAP Laser Applications).

	Initial position	**Position after correction**
Longitudinal	-7 mm	+2 mm
Lateral	+3 mm	-1 mm
Vertical	+5 mm	+2 mm
Rotation	6.3° CCW	6.3° CCW

The gel results were normalized to a TPS calculated dose using a region of homogenous dose in a slice without the presence of the fiducials or the fiducial support structure. Evaluation of the irradiated vials confirmed the linearity of the gel dose response for this batch of gel (R^2 = 0.98). An overlay of the 95% isosurface of the TPS calculated dose distribution and the measured dose distribution using gel showed good agreement (figure 3, left). The numbers of voxels inside the 95% dose level were 46586 and 45303 for the calculated and measured dose distribution, respectively. Further, the CTV volume was well centred inside the 95% isodose surface of the measured volume (figure 3, right). An increase of the R2 value was apparent in the region surrounding the fiducial support structure. This MRI read-out artefact typically corresponded to a relative dose increase of 25% in a radius of 1 cm around the structure compared to the TPS calculated dose distribution. However, this effect did not compromise the determination of the location of the 95% isodose surface as the fiducials were located centrally in the volume of interest.

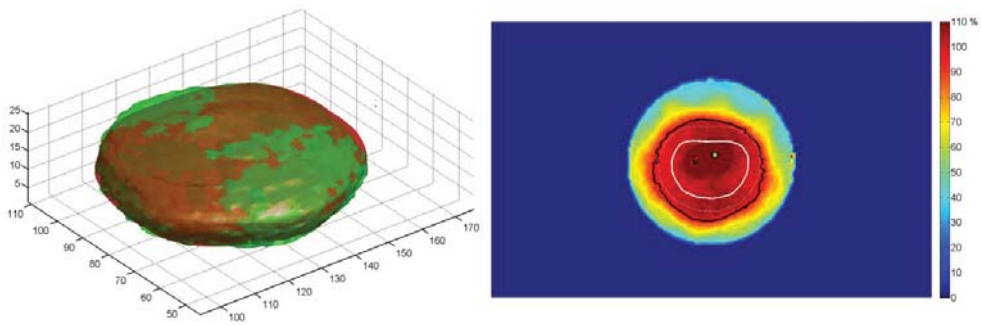

Figure 3. An overlay of the TPS calculated dose distribution (red) and the measured dose distribution (green) using alpha blending (left). Only the 95% isodose are shown. A 2D slice with both the measured and calculated 95% isodoses (black), as well as the CTV and PTV structures (white) are shown to the right.

4. Conclusions

This study showed that MRI based nPAG gel dosimetry can be used to verify setup correction procedures using implanted gold fiducials. For the case used in this pre-study, it was shown that the use of on-board imaging and integrated setup correction tools could be used to compensate for a deliberately introduced offset in CTV position. By expanding this study to include more patient cases, it should be possible to draw more general conclusions about the IGRT setup correction capabilities. This would be of value in order to determine the part of the PTV margin magnitude intended to account for inter-fractional movement of the prostate.

Acknowledgements

This study was financially supported by the Swedish Cancer Society.

References

[1] Hanks G E, Lee W R, Hanlon A L, Hunt M, Kaplan E, Epstein B E et al. 1996 Conformal technique dose escalation for prostate cancer: Biochemical evidence of improved cancer control with higher doses in patients with pretreatment prostate-specific antigen ≥10 ng/ml. *Int J Radiat Oncol Biol Phys* **35** 861-8

[2] Pollack A, Zagars G K 1997 External beam radiotherapy dose response of prostate cancer. *Int J Radiat Oncol Biol Phys* **39** 1011-8

[3] Zelefsky M J, Leibel S A, Gaudin P B, Kutcher G J, Fleshner N E, Venkatramen E S et al. 1998 Dose escalation with three-dimensional conformal radiation therapy affects the outcome in prostate cancer. *Int J Radiat Oncol Biol Phys* **41** 491-500

[4] Sorey M R, Pollack A, Zagars G, Smith L, Antolak J, Rosen I 2000 Complications from radiotherapy dose escalation in prostate cancer: preliminary results of a randomized trial. *Int J Radiat Oncol Biol Phys* **48** 635-42

[5] Balter J M, Lam K L, Sandler H M, Littles J F, Bree R L, Ten Haken R K 1995 Automated localization of the prostate at the time of treatment using implanted radiopaque markers: Technical fesibility. *Int J Radiat Oncol Biol Phys* **33** 1281-6

[6] Kupelian P A, Langen K M, Willoughby T R, Zeidan O A, Meeks S L 2008 Image-guided radiotherapy for localized prostate cancer: treating a moving target. *Semin Radiat Oncol* **18** 58-66

[7] HYPO-RT-PC Phase III study of HYPOfractionated RadioTherapy of intemediate risk localised Prostate Cancer, *http://www.controlled-trials.com/ISRCTN45905321*

[8] Vergote K, De Deene Y, Duthoy W, De Neve W, Achten E, De Wagter C 2004 Validation application of polymer gel dosimetry for the dose verification of an intensity-modulated arc therapy (IMAT) treatment. *Phys Med Biol* **49** 287-305

[9] Isbakan F, Ûlgen Y, Bilge H, Ozen Z, Agus O, Buyuksarac B 2007. Gamma Knife 3-D dose distribution near the area of tissue inhomogeneities by normoxic gel dosimetry. *Med Phys* **34** 1623-30

[10] Gustavsson H, Karlsson A, Bäck S Å J, Olsson L E 2003 MAGIC-type polymer gel for three-dimensional dosimetry: Intensity-modulated radiation therapy verification. *Med Phys* **30** 1264-70

[11] Ceberg S, Karlsson A, Gustavsson H, Wittgren L, Bäck S Å J 2008 Verification of dynamic radiotherapy: the potential for 3D dosimetry under respiratory-like motion using polymer gel. *Phys Med Biol.* **53** 387-96

[12] Karlsson A, Gustavsson H, Månsson S, McAuley K B, Bäck S Å J 2007 Dose integration characteristics in normoxic polymer gel dosimetry investigated using sequential beam irradiation. *Phys Med Biol* **52** 4697-706

[13] Karlsson A 2007 Characterization and clinical application of normoxic polymer gel in radiation therapy dosimetry. *Ph.D.-thesis, Lund University, Malmö*